Heritage Science

RESEARCH ARTICLE

Open Access

Trace element distribution in human cortical bone microstructure: the potential for unravelling diet and social status in archaeological bones

Kaare Lund Rasmussen[1*], George R. Milner[2], Thomas Delbey[1], Lilian Skytte[1], Niels Lynnerup[3], Jørgen Lange Thomsen[4], Simone Schiavone[5], Marielva Torino[6], Lars Agersnap Larsen[7] and Jesper Lier Boldsen[8]

Abstract

Variation in the trace element chemistry of cortical bone microstructure is delineated for interred and non-interred human femora. This was done to investigate the range of element concentrations that might occur within single bones, specifically the original laminar bone and later osteons, and its potential for investigating chemical life histories. To do so, femora were chosen from individuals who experienced quite different ways of life over the past two millennia. The distributions of Sr, Ba, Cu, and Pb, mostly in partial (early) and complete (late) osteons, in cross-sections of proximal femora were characterized through Laser Ablation Inductively Coupled Plasma Mass Spectrometry. Absolute calibrations of these data were obtained using solution Inductively Coupled Plasma Mass Spectrometry on adjacent dissolved bulk samples. Chemical life histories were approximated by classifying bone microstructure into four categories: laminar bone and 1st, 2nd, and 3rd generation osteons. This four-part sequence, on average, charts the temporal dimension of an individual's life. Consistent with recent studies of medieval bones, Sr and Ba are thought to be mainly responsive to diet, presumably related to the consumption of mostly locally produced food, while Cu and Pb do the same for heavy metal exposure often attributable to social status or occupation. No systematic differences in these elements were found between interred and non-interred individuals. The effect of diagenesis on interpretations of life histories based on archaeological bone, therefore, are minimized by plotting element concentrations across cortical bone cross-sections.

Keywords: Osteons, Trace element chemistry, LA-ICP-MS, Sr, Ba, Cu, Pb, Cortical bone, Diet, Provenance, Social status

Introduction

This study builds on earlier work that involved the elemental mapping of microscopic features visible in cortical bone cross-sections to identify signals attributable to diagenesis, as opposed to those reflecting life experiences, notably dietary composition and residential location [1]. These results parallel those of Swanston et al. [2, 3] and Choudhury et al. [4] who characterized the distributions of Sr and Pb by means of synchrotron radiation in long bone cross sections from archaeological skeletons that were about two centuries old, and the work of Pemmer et al. [5] and Wittig et al. [6] who examined microstructural variation in trace element concentrations in modern bones. Collagen in the bone microstructure of Dutch whalers interred in Spitsbergen has likewise been investigated for stable isotopes by Koon and Tuross [7].

The present investigation expands on these recent studies by reporting absolute concentrations of the elements Sr, Ba, Cu, and Pb in μg g^{-1} in cortical bone

*Correspondence: klr@sdu.dk
[1] Cultural Heritage and Archaeometric Research Team (CHART), Department of Physics, Chemistry and Pharmacy, University of Southern Denmark, Campusvej 55, 5230 Odense M, Denmark
Full list of author information is available at the end of the article

cross sections. It provides the elemental composition of between 96 and 181 osteons in 6 femora, two from individuals that were never buried and four from medieval to post-medieval skeletons interred in soil for centuries. In addition to what can be said about the lives of past people, this approach contributes to an understanding of the range of variation that occurs in the elemental composition of the inorganic fraction of bone in single individuals. It does so by examining microscopic bone structures formed at different times in a person's life. Bulk samples, by far the most common way of characterizing bone composition, combine many such structures, so they track neither the variation present in single individuals nor changes that take place during a lifetime.

Samples were selected to secure non-interred and interred bones from different contexts to determine if buried bones yielded explicable results, identify any diagenetic effects if present, and assess whether old bones yield information of life history significance. Non-interred individuals were represented by the youngest and the oldest skeletons in the sample. The excavated skeletons were from two medieval and post-medieval Danish towns—Ribe and Viborg—that are about 130 kms from one another.

The distributions of four elements—Sr, Ba, Cu, and Pb—in cross-sections of human femoral cortical bone provide information useful for reconstructing life histories from archaeological skeletal remains. That is done through characterizing various aspects of bone microstructure in terms of their trace element composition. Two elements, Fe and Mn, are included for comparative purposes as they are generally regarded as being strongly affected by diagenesis [1, 8–10].

Bone microstructure, composition, and life histories

The work reported here is structured around distinguishing early from late forming bone visible microscopically and characterized through bone chemistry in cortical bone cross-sections. The earliest bone visible in the cross-sections is laminar bone laid down, for the most part, during the juvenile years. Later remodelling takes place through bone destruction and deposition as new osteons (Haversian systems) are formed [11, 12]. When sectioned transversely, osteons are visible as concentric layers of mineralized tissue and embedded osteocytes that surround blood vessels. In bone cross-sections, osteons appear as circular, oval, or irregular structures, depending on whether they were bifurcating where cut and their orientation relative to the sectioning plane. Regardless of their shape, they have a distinctive structure, hence appearance, even when partly destroyed by later osteons.

New osteons are continually formed throughout life as bones remodel in response to mechanical forces acting on the skeleton [13, 14]. This process occurs through osteoclasts destroying old bone, and osteoblasts laying down new bone. Over time, the original laminar bone and earlier osteons are progressively obliterated through the formation of new osteons, which continues until death occurs. Eventually all that can be seen in bone cross-sections are fragmentary and complete osteons. This continual remodelling forms the basis of efforts to assess the age of adults from counts of complete and partial osteons, and to a lesser extent changes in osteon size [14–19]. The considerable variation that exists among individuals and observer error in the counting process, however, introduce great uncertainty about age estimates based on what can be seen in cortical bone cross-sections.

An osteon's crystalline structure is formed in equilibrium with elements circulating in the blood at that time. They include divalent cations that can substitute for Ca^{2+} in the hydroxyapatite that makes up the inorganic fraction of bone. Modern humans in developed nations enjoy a diet composed of food from diverse sources, often from places as distant as other continents. What is consumed differs from one person to the next, depending on the local supermarket's supply chain and dissimilar travel histories. It is therefore expected that the trace-element composition of individual osteons, which are formed at various points in a person's life, would vary considerably.

In the past, individual mobility and food diversity were limited relative to what they are today, at least for most people. In medieval Denmark, for example, most villagers for much, if not all, of their lives rarely travelled farther than 10–20 kms, and then often only to a nearby market town [20, 21]. There they would have exchanged what they had produced, including food, for tools and other necessities that could also have included locally grown food. Yet that is not the entire story because some fraction of the population moved far enough one or more times during their lifetimes to encounter geologically settings that would result in different elemental and isotopic signatures in their skeletons. People who periodically changed their places of residence presumably included those in the lowermost socioeconomic strata, as well as specialists whose services were much in demand (e.g., skilled stone masons) and members of the nobility along with their servants. Identifying how many people moved and how often they did so represent major challenges when characterizing the life experiences of people in the past, including medieval Europe.

Bone chemistry as a means of making inferences about the diets and movement of people who lived in the past has had a long history in archaeology. Although

it is widely accepted that much can be learned through analyses of long-buried skeletons, there remain concerns about whether the original chemical composition of bone is modified or obscured altogether by postmortem processes, or diagenesis [22–32]. Diagenetic change can result in the addition or removal of trace elements after burial, and not all elements are expected to behave similarly. This concern—and there are indeed reasons to be troubled by diagenesis—led to a general dismissal of the use of trace-element chemistry for dietary purposes in the 1990s. But it is also true that, with proper pre-treatment, some elements, notably Sr and Ba, are thought to yield reliable dietary and provenance information [1, 29, 33–37]. Furthermore, Pb and Cu can reveal much about environmental exposure to these elements, including the social position of people in the past [37–41].

Materials

Skeletons

Bone samples were obtained from a non-interred skeleton from the 18th or 19th centuries AD, one skeleton ca. 2000 years old that was probably never buried, and four medieval or post-medieval skeletons from two Danish cemeteries. The six specimens have been selected from 90 individuals examined so far as a proof of concept for this analytical procedure. The skeletal remains were purposefully chosen to encompass different geographical areas, ranging from Denmark, Italy, to Israel, although the focus is on the Danish archaeological skeletons. The remains also span a long interval of time, up to two millennia. The six individuals are as follows.

1) A middle-aged male from Maiori, Italy, from the 18th or 19th centuries. Not-interred. Naturally mummified in a hot and dry church attic, and recently deposited with other bones in a tightly sealed aluminium box. Slightly osteoporotic (KLR-11742).
2) The Holy Relics attributed to the Apostle St. James the Lesser (S. Giacomo) from the Church of the Twelve Holy Apostles in Rome, Italy. According to tradition not-interred (C94/KLR-11251).
3) A 45–55-year-old medieval to post-medieval male excavated from the Lindegaarden cemetery in Ribe, Denmark (ASR13, X1256/KLR-10810).
4) A 37–47-year-old post-medieval female excavated from the Lindegaarden cemetery in Ribe, Denmark. Signs of syphilis (ASR13, X1029/KLR-10831).
5) A 24–30-year-old medieval male excavated from Viborg Cathedral, Denmark (VSM C810 X27/KLR-7292).
6) A 20–24-year-old medieval female from Viborg's Sct. Morten cemetery, Denmark (VSM 09715, X1050/KLR-11500).

The bones from the two never buried individuals had intact surfaces with no visible evidence of postmortem degradation. The four skeletons from archaeological excavations were typical of better preserved Danish medieval and early modern skeletons. There was no externally visible evidence, such as abnormal surficial erosion, that might lead one to suspect that the bones had undergone severe diagenesis. The sexes and ages of these individuals, as well as the one from Maiori, were estimated by experience-based methods [42]. For the archaeological skeletons, there were no metallic objects, such as swords or knives, in the graves that might alter the bone composition by being located nearby.

Bone samples

Two bone samples were taken from proximal femoral shafts just distal to the lesser trochanter. They were located immediately adjacent to one another, with one used for solution Inductively Coupled Plasma Mass Spectrometry (ICP-MS) and the other to obtain cross-sections for chemically characterizing bone microstructure through Laser Ablation ICP-MS (LA-ICP-MS).

A clean surface for all bone samples was ensured by conducting the work on two sheets of Al foil. The lower sheet, replaced as necessary, prevented contamination from the table. The upper sheet—the one that came in direct contact with the bone—was replaced after each femur was sampled. The person who obtained the samples wore protective gear that included lab coat; disposable latex gloves, discarded after each sample; dust mask; and hairnet. Gloves were replaced between the decontamination and sampling steps, as well as between samples.

Two bone samples next to each other were obtained using a Dremel Multipro drill with a stainless-steel sawblade. The sawblade, which was the only part of the tool that came into contact with the bone, was cleaned after each use with MilliQ-water (Merck Millipore, Billerica, MA, USA), and it was then dried by heating in an ethanol flame. This rinsing step, which is standard procedure in our lab, prevents contamination from dust or leftover material from the previous specimen. Heating eliminates contamination with Hg, an element measured separately but not reported here. Once cut from the femora, one intact sample was mounted in Struers' Epoxy resin, ground with grades 500 and 1200 SiC, and polished to a 9, 3, and finally 1 μm diamond finish. The sample was then photographed using optical microscopy. It was the sample subsequently used for the LA-ICP-MS analysis. The second block of bone had all surface areas removed down to 1–2 mm, and was subsequently subjected to dissolution and ICP-MS. In a previous study, it was shown that exposed surfaces of medieval Danish bones are

typically degraded physically and chemically, but 1 mm is more than twice the depth of the postmortem changes [1]. Removing bone from all surfaces of the bone block not only took into account degraded bone on once-exposed surfaces, but also possible contamination from handling.

Analytical techniques

Laser ablation ICP-MS

Laser Ablation was performed with a CETAC LXS-213 G2 equipped with a NdYAG laser having a wavelength of 213 nm. A circular aperture of 10 μm was used, and the shot frequency was 20 Hz. The spatial concentrations of elements for each cross-section were mapped using 100 horizontal lines. Each line was scanned at 10 μm s^{-1}, typically taking some 250 s to complete. Each scan line was preceded by a 10 s gas blank. The helium flow was 600 mL min^{-1}. Laser operations were controlled by DigiLaz G2 software from CETAC.

The ICP-MS analyses were undertaken with a Bruker Aurora M90. The radiofrequency power was 1.30 kW, plasma Ar gas flow rate was 16.5 L min^{-1}, auxiliary gas flow rate was 1.65 L min^{-1}, and sheath gas flow rate was 0.18 L min^{-1}. The following isotopes were measured without skimmer gas: ^{55}Mn, ^{57}Fe, ^{63}Cu, ^{88}Sr, ^{137}Ba, and ^{208}Pb. No interference corrections were applied to the selected isotopes. The dwell time on each peak was 10 ms, and the total scan time was ca. 360 ms. The LA-ICP-MS data for each element was calibrated into absolute concentrations by taking an average over a large part of the scanned area, measuring several square mm, and then normalizing it to the bulk concentration as determined through solution ICP-MS bulk analysis on an adjacent *ca*. 20 mg sample.

Solution ICP-MS

Bulk samples of compact tissue were analysed by solution ICP-MS. The resulting data were used to calibrate the LA-ICP-MS measurements, as described above.

Inductively Coupled Plasma Mass Spectrometry (ICP-MS) was used to collect data on 16 elements, but only Mn, Fe, Cu, Sr, Ba, and Pb are reported here. The ICP-MS samples each consisted of ca. 20 mg of bone. A stainless-steel spoon was used to handle the samples, and between each sample it was rinsed in MilliQ-water (Merck Millipore, Billerica, MA, USA) and heated in an ethanol flame. After a sample was weighed, it was transferred to a clean 50 mL disposable polypropylene centrifuge tube. Samples in their tubes were dissolved by adding 2 mL of conc. 65% ICP-MS grade HNO_3 and 1 mL of conc. 30% ICP-MS grade H_2O_2 (TraceSELECT® Fluka). The tube's lid was then loosely fitted before it was placed on a shaking table for over 3 h. The amount of H_2O_2 consumed during the dissolution process depended on the organic compounds, such as collagen, present in the sample. Therefore, an excess of H_2O_2 was added. Surplus H_2O_2 was removed by adding 400 μL of conc. 38% ICP-MS grade HCl (PlasmaPURE Plus® SCP Science), after which the tube, with loosely fitted lid, was placed on a shaking table overnight.

Samples were diluted quantitatively to 10 mL with MilliQ-water, and they were then filtered through a 0.45 μm PVDF Q-Max® RR Syringe filter into a 15 mL disposable polypropylene centrifuge tube. Further quantitative dilution was done in the 15 mL tubes according to the concentrations of specific samples. Normally a 3 mL sample solution and 9 mL of MilliQ-water were used when doing so. Diluted samples thus acquired acid concentrations of ca. 1%, which is well suited for ICP-MS analysis.

The ICP-MS analyses were carried out using a Bruker ICP-MS 820 fitted with a frequency matching RF-generator and a Collision Reaction Interface (CRI) operated with either helium or hydrogen. Samples were introduced using a Bruker SPS3 autosampler and an OneFast flow injection inlet system. The radiofrequency power was 1.40 kW, plasma gas flow rate was 15.50 L min^{-1}, auxiliary gas flow rate was 1.65 L min^{-1}, sheath gas flow rate was 0.12 L min^{-1}, and nebulizer gas flow rate was 1.00 L min^{-1}. Several isotopes were measured without skimmer gas: ^{55}Mn, ^{88}Sr, ^{137}Ba, and ^{208}Pb. The CRI Reaction System was used for Fe and Cu because interferences with polyatomic species produced by a combination of isotopes from the argon plasma, reagents, and bone matrix were theoretically possible. ^{56}Fe was measured with hydrogen as skimmer gas, and ^{63}Cu with helium. A mixture of ^{45}Sc, ^{89}Y, and ^{159} Tb was added continuously as an internal standard. The dwell time on each peak was between 5 and 20 ms. Five replicate analyses were made of each dissolved bone sample, and each replicate was measured with 30 mass scans. An ICP multi-element standard solution XXI for MS from Merck was prepared in 1% HNO_3 at 6 concentrations (0.1, 1, 10, 20, 100, and 200 μg L^{-1}). For each element, three standards were selected to fit the appropriate sample concentration range. For the main element Ca, three standards of 100, 200, and 250 μg L^{-1} were used (Fluka TraceCert® ICP Standard). Elements showing higher than expected concentrations had count rates attenuated automatically by the MS detector. Blank samples of MilliQ-water and 1% HNO_3 were run before the standard blank to ensure that pollutants were not lingering in the system at start up. Between each bone sample a blank sample of 1% HNO_3 was analysed to rinse the system and avoid possible memory effects. Each day an in-house standard sample made from a homogenized medieval bone was analysed along with the samples to monitor the analytical

system's overall performance. An international modern bone standard, NIST SRM-1486, was analysed along with the study samples. Concentrations below the limit of quantification (LOQ) are reported as < LOQ. The LOQ was estimated as 10 times the standard deviation over the detection limit, where the standard deviation was a mean of standard deviations measured over a *ca*. half-year period with one or two weekly runs. The LOQ values were calculated as 0.51 μg g^{-1} for Mn, 13.5 μg g^{-1} for Fe, 0.72 μg g^{-1} for Sr, 2.56 μg g^{-1} for Cu, 0.49 μg g^{-1} for Ba, and 0.49 ng g^{-1} for Pb.

Bone microstructure identification

Elemental distribution maps

Two examples of LA-ICP-MS element mapping are provided in Fig. 1. The Sr distribution plot for a femoral cross-section from a Danish archaeological skeleton, Viborg KLR-11500, can be seen in Fig. 1a; the same for a non-interred, but centuries old, femur from Maiori, KLR-11742, is shown in Fig. 1b. The endosteal surface of the medieval bone, visible in the lower centre of Fig. 1a, is relatively high in Sr. This concentration of Sr might be attributable to the presence of newly mineralized bone yielding a sufficiently different chemical signature to be picked up on the cross-section plots. Similar thin Sr-rich zones are routinely visible on the outer edges of bone cross-sections, again perhaps attributable to new bone formation or a mineralization of the periosteum and perforating Sharpey's fibres [1, 43, 44]. It is apparent from the interiors of these specimens that as osteons form throughout a person's life the amount of Sr incorporated into the crystalline fraction of the bone can vary considerably.

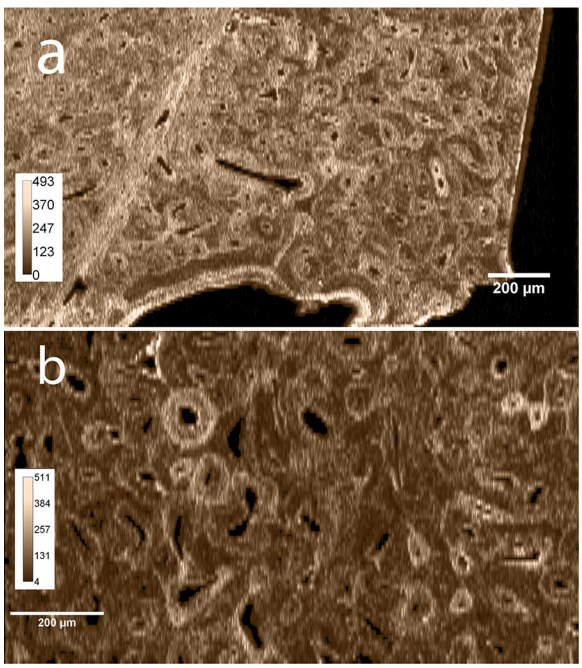

Fig. 1 Two examples of Sr-distribution maps: **a** a medieval or post-medieval individual from Viborg X1050/KLR-11500; and **b** a non-interred middle-aged male from Maiori, KLR-11742. The lighter the colour, the higher the Sr-concentration; Sr-concentration scales have been inserted, and values are given in μg g^{-1}

Osteon classification

Osteon outlines were identified based on optical images of embedded polished bone segments prior to LA-ICP-MS measurement, as well as the element distribution maps produced, mainly for Sr and Pb. For each osteon, the area inside the cement line, but outside the central Haversian canal, was marked manually with a pen on a digital writing pad. An optical microscopic image and the accompanying hand-drawn osteon outlines are shown in Fig. 2 for the ca. 2000 year old Apostle/KLR-11251 skeleton.

Colour codes in Fig. 2b illustrate a classification of bone microstructure according to the relative time of its formation. What is of interest is the superposition of microstructural features, from earliest to latest. For the osteons, it is important to recognize that the sequence from early to late does not imply anything about the actual amount of time that elapsed between their formation. It is, instead, merely a relative temporal ordering of osteons. The classification provides a rough approximation of an individual's chemical life history from single bone cross-sections. Any patterning in the results, to the extent it is interpretable within the cultural context of the skeletons, will necessarily be muddier than if the absolute timing of osteon sequences were known, or indeed knowable.

In Fig. 2b, yellow refers to the original laminar bone laid down when the person was young. Dark green osteons, referred to here as 1st generation osteons, penetrated the laminar bone, and they were, in turn, cut by at least one other osteon. Osteons in magenta, designated 2nd generation, cut through at least one previous osteon, and they were themselves cut by at least one other osteon that formed later in life. Turquoise osteons, here called 3rd generation osteons, were intact at the time of death; that is, they were not cut by a later forming osteon. The hand drawn outlines in Fig. 2b do not always seem to conform to the four categories, but if the optical image in Fig. 2a is taken into account the classification is clear. Once again, the microstructure classification is a relative chronology, not an absolute one, but it captures a general tendency for the three osteon types to be ordered from early to late in an individual's life, following the initial formation of laminar bone.

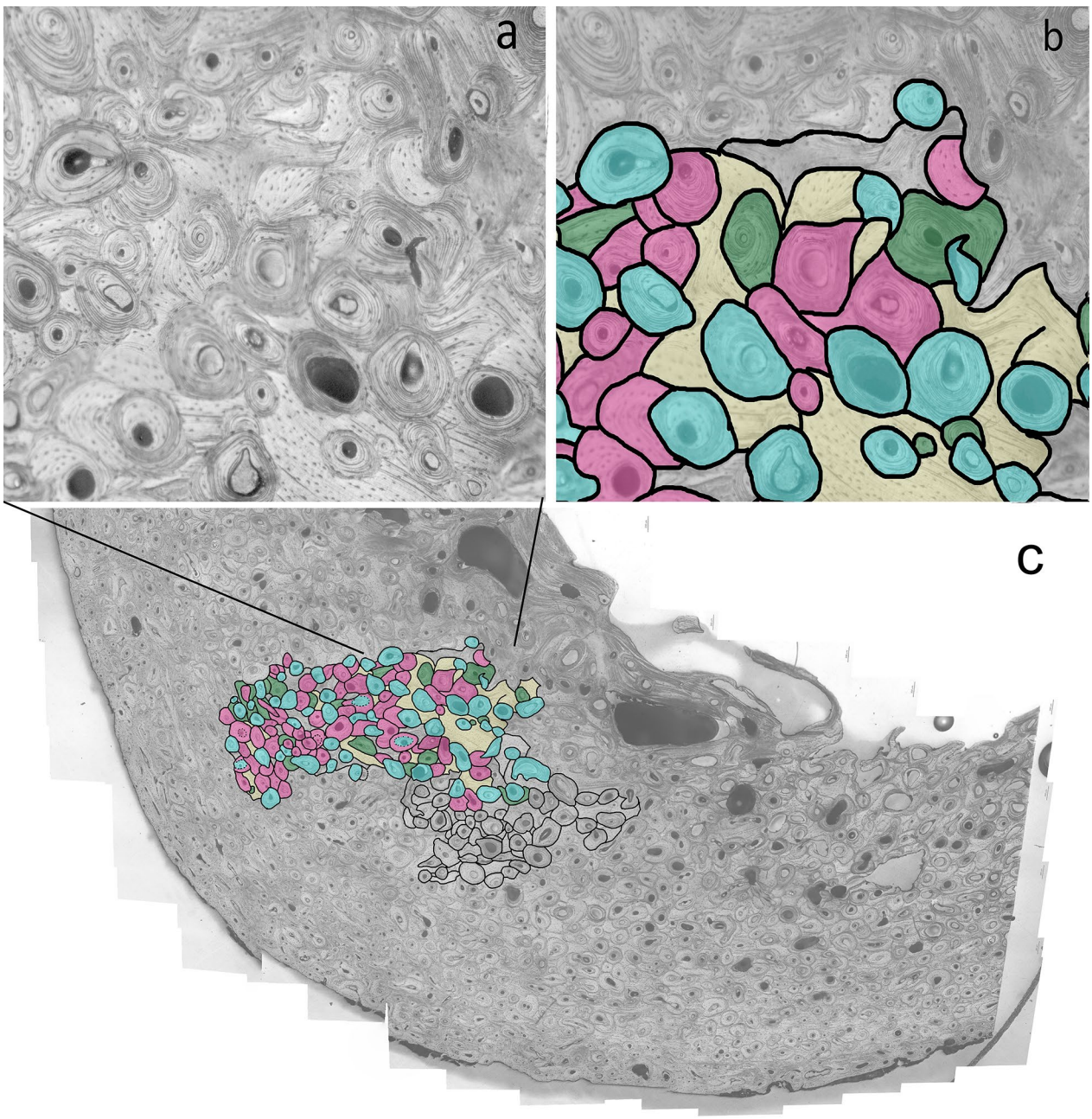

Fig. 2 Cross-section from the femur of the Apostle/KLR-11251, showing remnants of the original laminar bone and later osteons: **a** optical microscope image of polished cortical bone; **b** image with bone microstructure classified. Yellow is laminar bone, and dark green, magenta, and turquoise designate 1st, 2nd, and 3rd generation osteons, respectively; and **c** the entire group of osteons measured in the bone

All mapped osteons are shown in Fig. 2c for the apostle. It can be seen that bone near the outer and inner surfaces of the cortex was avoided, well beyond the 1 mm conservative estimate for possibly degraded bone from medieval Danish cemeteries [1]. For all specimens, regardless of whether they were ever buried or not, once-exposed surfaces were avoided.

Element concentrations were estimated as arithmetic means and standard deviations of the pixel values in each of the four bone microstructure categories (Figs. 2b and c). For the osteons, the pixels between the cement line and the central Haversian canal were used when estimating mean element concentrations, excluding pixels immediately adjacent to the exterior line or interior

canal. Doing so eliminated the confounding effects of element concentrations at the cement lines and Haversian canal margins [1, 5], as well as the possibility that material within the canals was inadvertently measured. This step was important because osteons, which were often incomplete, differed in the amount of edge zone (cement lines plus canal margins) present relative to the lamellae that form the bulk of an intact osteon.

Results

The concentrations of Sr, Ba, Cu, and Pb for each of the scored structures, laminar bone, 1st, 2nd, or 3rd generation osteons, as well as their coordinates in the cross-sections, are provided in Additional file 1. Between 96 and 181 osteons were analysed in the six femora. Depending on the age when the individual died, there are different proportions of the four microstructure categories. One individual has no laminar bone in the part of the cortical bone examined, although 1st, 2nd, and 3rd generation osteons are all present. Others have only 2nd and 3rd generation osteons in the areas selected for study.

Evaluation of the data set

Because this way of producing and presenting trace-element data for bones is new, a thorough statistical evaluation is warranted. It is especially important to determine if signs of diagenesis can be detected, which is why Mn and Fe are included in Table 1. If there are such signs, they should be seen only in the four excavated skeletons, not in the two bones that had never been buried in soil.

Table 1 Element concentrations are summarized for six femora, including for each sample maximum and minimum values, arithmetic means, standard deviations (SD), all in µg g^{-1} and relative standard deviations (RSD) in %

		Mn	Fe	Cu	Sr	Ba	Pb
Apostle/KLR-11251 (n=166)	Minimum (µg/g)	1.60	12.9	0.841	69.7	1.58	10.9
	Maximum (µg/g)	3.12	18.9	7.19	167.0	8.62	90.8
	Mean (µg/g)	2.14	14.8	2.11	121.2	3.97	32.6
	SD (µg/g)	0.232	0.917	0.871	17.4	0.935	14.5
	RSD (%)	0.108	0.0619	0.411	0.143	0.235	0.443
Maiori/KLR-11742 (n=176)	Minimum (µg/g)	6.02	70.8	8.41	24.9	1.04	6.49
	Maximum (µg/g)	8.73	97.3	44.9	322	12.9	56.0
	Mean (µg/g)	6.57	76.7	17.0	96.0	3.90	20.6
	SD (µg/g)	0.41	4.06	5.28	59.8	2.20	9.67
	RSD (%)	0.0615	0.0527	0.311	0.622	0.562	0.468
K1256/KLR-10810 (n=181)	Minimum (µg/g)	6.06	31.1	4.71	72.9	3.20	4.14
	Maximum (µg/g)	7.43	39.6	32.3	854	16.7	16.6
	Mean (µg/g)	6.54	35.3	10.9	299	7.78	7.34
	SD (µg/g)	0.31	1.32	3.99	134	2.36	1.93
	RSD (%)	0.0471	0.0373	0.365	0.446	0.303	0.262
K1029/KLR-10831 (n=116)	Minimum (µg/g)	386	346	7.61	52.8	4.23	13.5
	Maximum (µg/g)	7245	487	60.7	708	51.3	213
	Mean (µg/g)	1230	404	21.8	303	22.7	52.7
	SD (µg/g)	1194	19.6	10.1	178	12.5	32.5
	RSD (%)	0.966	0.0483	0.461	0.586	0.551	0.613
810C27/KLR-7292 (n=96)	Minimum (µg/g)	37.1	407	5.62	160	11.0	3.47
	Maximum (µg/g)	41.0	479	28.8	561	44.8	13.0
	Mean (µg/g)	38.8	434	11.0	343	22.7	5.83
	SD (µg/g)	0.753	13.6	4.08	81.8	5.28	1.45
	RSD (%)	0.0193	0.0312	0.371	0.237	0.231	0.247
X1050/KLR-11500 (n=154)	Minimum (µg/g)	17.1	64.5	1.50	58.7	2.33	0.503
	Maximum (µg/g)	87.8	213	5.26	299	9.40	2.06
	Mean (µg/g)	29.8	81.6	2.81	158	5.12	0.786
	SD (µg/g)	13.1	13.6	0.636	56.7	1.62	0.221
	RSD (%)	0.440	0.166	0.225	0.358	0.315	0.280

Singular outliers have been omitted in this calculation

(See figure on next page.)

Fig. 3 Boxplot of the distributions of the osteon chemistry of two archaeological but non-interred individuals, the Apostle/KLR-11251 and Maiori/KLR-11742, expressed as µg/g for each element. The p-values at the top of the diagram are Dunn's multiple comparison tests with alpha = 0.05 calculated after the one-way ANOVA analysis. The boxes indicate the extent between Q1 and Q3; the error bars indicate limits of Q1 + 1.5*IQR; the red crosses are the means; lines inside boxes are the medians; open circles are outliers in the range 1.5*IQR and 3 standard deviations; closed circles are outliers over 3 standard deviations from the mean; and crosses are extreme outliers according to the 3*IQR rule

Table 1 lists summary bone chemistry data for the six femora, and Additional file 2 provides a Spearman correlation matrix. Means, relative standard deviations, and relative standard deviations (RSD) are given for each bone microstructure category in Additional file 3, as are the results from Dunn's multiple comparison tests from Kruskal–Wallis one-way ANOVA.

Non-interred samples

In the two bones that were never buried, Maiori/KLR-11742 and Apostle/KLR-11251, the concentrations of Mn, Ba, and Pb are similar, relative to the range of values in the entire group of specimens (Table 1). Iron and Cu are noticeably higher in Maiori/KLR-11742, while Sr is higher in Apostle/KLR-11251. The person from Maiori, KLR-11742, has higher Cu concentrations than the much older Apostle/KLR-11251. Nevertheless, all elemental concentrations measured here are still within the range of concentration values reported for modern Taiwanese and Polish bones [45, 46]. The Spearman correlation matrix indicates a different situation for these two individuals (Additional file 2). For Maiori/KLR-11742, there are strong positive correlations between Sr, Ba, Pb, and Cu ($r > 0.8$). In contrast, only one strong correlation was found in Apostle/KLR-11251, and it was between Sr and Ba ($r = 0.8$).

At the time of sample collection, it was thought that the Maiori/KLR-11742 femur was from an individual with osteoporosis, so old age might be why only 2nd and 3rd generation osteons were observed. In the Apostle/KLR-11251 femur, many of the Pb, Ba, Sr, and Cu concentrations significantly increase from the initial laminar bone through 1st, 2nd, and 3rd generation osteons (Fig. 3). For Maiori/KLR-11742, there are significant increases for all elements from the 2nd to 3rd generation osteons.

Archaeological samples from Ribe, Denmark

The two archaeologically derived skeletons from Ribe differ in their bone chemistry (Additional file 3). The concentrations of elements in X1256/KLR-10810 are reasonably close to those of the two non-interred samples, except for Sr which is higher (average of 299 µg g^{-1}). In Ribe X1029/KLR-10831, all concentration values are higher than those in the unburied samples, especially for Mn but also Fe and Ba. Copper and Pb are higher than in the non-interred individuals, but they are within the range of archaeological Danish skeletons reported elsewhere [37]. The Spearman correlation matrix shows that in X1256/KLR-10810 there are strong correlations between Sr and Ba ($r = 0.94$), as well as Cu and Pb ($r = 0.79$) (Additional file 2). For X1029/KLR-10831, Mn, Sr, and Ba are strongly correlated ($r \geq 0.8$), as are Pb with Sr, Ba, and Cu ($r \geq 0.8$).

Only 2nd and 3rd generation osteons were visible in the sampled area of X1256/KLR-10810, while 1st, 2nd, and 3rd generation osteons were seen in X1029/KLR-10831. Average values of Sr, Ba, Cu, and Pb are significantly higher in 3rd than in 2nd generation osteons in X1256/KLR-10810, and variation coefficients are similar (Table 1, Fig. 4). In the X1029/KLR-10831 femur, mean concentrations of the four elements are about the same in the first two osteon categories, but are usually significantly higher in the 3rd generation osteons (Fig. 4). Variation coefficients are high for Mn in all three osteon categories, much more so than for the other Ribe skeleton (Additional file 3).

Archaeological individuals from Viborg, Denmark

Elemental distributions in the two Viborg femora, excavated from different cemeteries, are quite different from one another. In X27/KLR-7292, the Mn, Fe, Sr, and Ba concentrations are high, and variation coefficients are low (Table 1, Additional file 3). The values tend to resemble those in X1029/KLR-10831 from Ribe more closely than they do in the two unburied bones from different contexts. Of the same four elements in X1050/KLR-11500, only Mn is much higher than the concentrations in both unburied bones. Turning to Cu and Pb, the concentrations in X27/KLR-7292 are higher than those in X1050/KLR-11500. The mean values of Cu for the Viborg femora fall within the range of those for the unburied bones, but those for Pb are lower than what was found for the never buried bones. The Spearman correlation matrix shows one strong correlation in X27/KLR-7292 between Ba and Sr ($r = 0.89$) (Additional file 2). In X1050/KLR-11500 there are strong correlations of Sr with Cu and Ba, as well as Cu with Pb and Ba ($r \geq 0.7$) (Additional file 2).

All four microstructure categories were represented in the Viborg samples, but there were less than 10 scored areas in each of the laminar bone and 1st generation osteon categories in these femora (Fig. 5). For both X27/KLR-7292 and X1050/KLR-11500, the Sr, Ba, Cu, and Pb

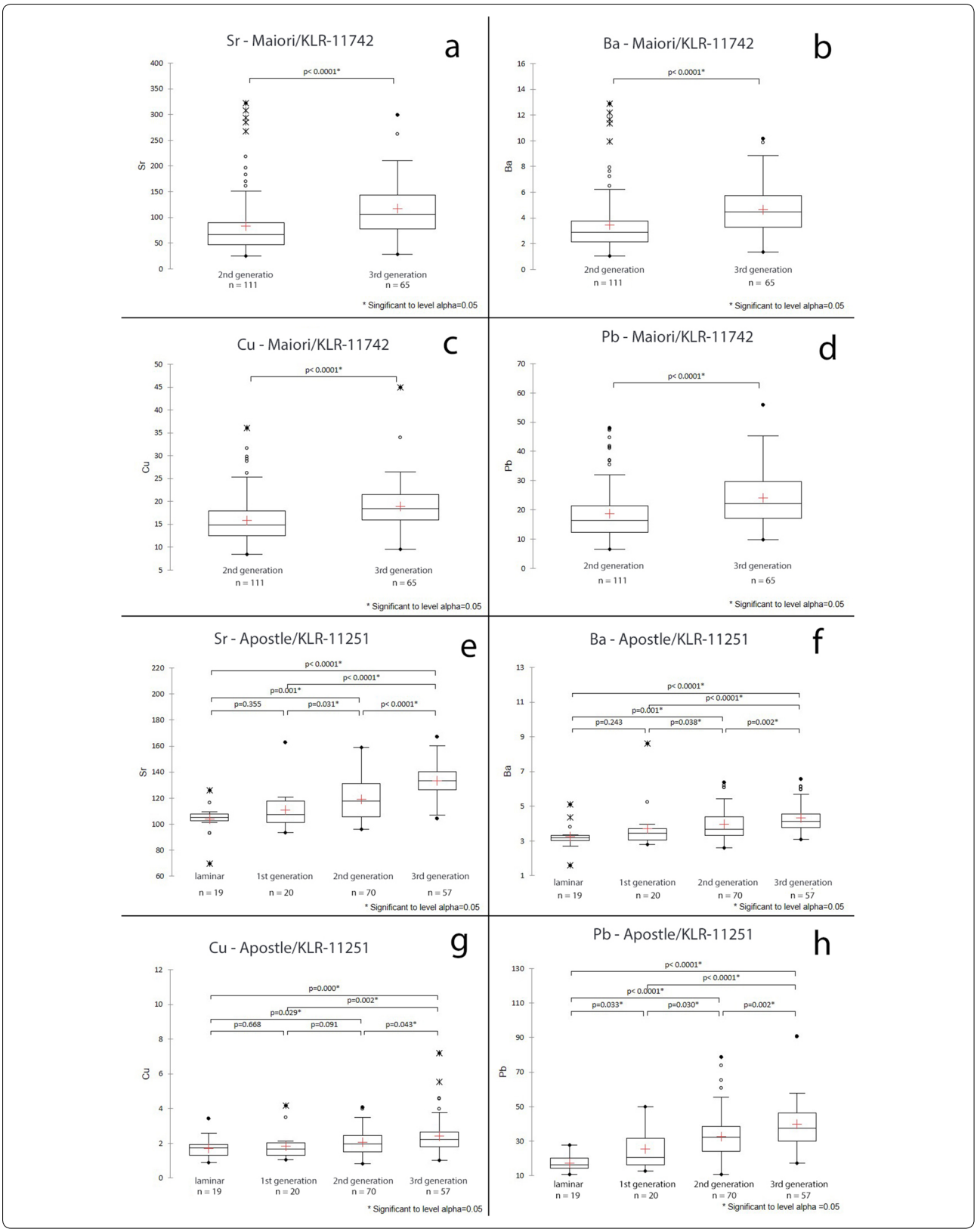
Sr - Maiori/KLR-11742
a
p< 0.0001*
Sr
2nd generatio
n = 111
3rd generation
n = 65
* Singificant to level alpha=0.05
Ba - Maiori/KLR-11742
b
p< 0.0001*
Ba
2nd generation
n = 111
3rd generation
n = 65
* Significant to level alpha=0.05
Cu - Maiori/KLR-11742
c
p< 0.0001*
Cu
2nd generation
n = 111
3rd generation
n = 65
* Significant to level alpha=0.05
Pb - Maiori/KLR-11742
d
p< 0.0001*
Pb
2nd generation
n = 111
3rd generation
n = 65
* Significant to level alpha=0.05
Sr - Apostle/KLR-11251
e
p< 0.0001*
p< 0.0001*
p=0.001*
p=0.355
p=0.031*
p< 0.0001*
Sr
laminar
n = 19
1st generation
n = 20
2nd generation
n = 70
3rd generation
n = 57
* Significant to level alpha=0.05
Ba - Apostle/KLR-11251
f
p< 0.0001*
p< 0.0001*
p=0.001*
p=0.243
p=0.038*
p=0.002*
Ba
laminar
n = 19
1st generation
n = 20
2nd generation
n = 70
3rd generation
n = 57
* Sigificant to level alpha=0.05
Cu - Apostle/KLR-11251
g
p=0.000*
p=0.002*
p=0.029*
p=0.668
p=0.091
p=0.043*
Cu
laminar
n = 19
1st generation
n = 20
2nd generation
n = 70
3rd generation
n = 57
* Significant to level alpha=0.05
Pb - Apostle/KLR-11251
h
p< 0.0001*
p< 0.0001*
p< 0.0001*
p=0.033*
p=0.030*
p=0.002*
Pb
laminar
n = 19
1st generation
n = 20
2nd generation
n = 70
3rd generation
n = 57
* Significant to level alpha =0.05

(See figure on next page.)

Fig. 4 Boxplot of the distributions of the osteon chemistry of two archaeological interred individuals from Ribe Denmark, X1256/KLR-10810 and X1029/KLR-10831, expressed as µg/g for each element. The p-values at the top of the diagram are Dunn's multiple comparison tests with alpha = 0.05 calculated after the one-way ANOVA analysis. The boxes indicate the extent between Q1 and Q3; the error bars indicate limits of Q1 + 1.5*IQR; the red crosses are the means; lines inside boxes are the medians; open circles are outliers in the range 1.5*IQR and 3 standard deviations; closed circles are outliers over 3 standard deviations from the mean; and crosses are extreme outliers according to the 3*IQR rule

concentrations are higher in 3rd than in 2nd generation osteons, often significantly so (Additional file 3).

Sr and Ba relationship

Concentrations of Sr and Ba for individual osteons are positively correlated with one another in all individuals, regardless of their original cultural context or postmortem histories (Fig. 6). Correlation coefficients between Sr and Ba (Additional file 2) vary from one individual to the next but are reasonably high for biological systems. The highest correlations ($r^2 = 0.98$) were in a never buried skeleton, Maiori/KLR-11742, and one of the archaeological skeletons from Ribe, X1029/KLR-10831. The lowest correlation is found in the Apostle (KLR-11251, $r^2 = 0.30$). The Ba/Sr ratios for all individuals and all microstructure categories are listed in Table 2.

In general, positive correlations between Sr and Ba in different microstructure categories could have been caused by changes in food sources or environmental exposure during an individual's life. Whatever took place, Sr and Ba covary in a relatively fixed manner. The strong relationship between Sr and Ba in multiple individuals from different locations and, especially, postmortem contexts indicates that these elements are incorporated into the hydroxyapatite crystal in a regular manner with respect to one another. That increases confidence in the use of these elements as chemical indicators of life experience. Alternatively, the correlation between Sr and Ba could result from strong metabolic control of the formation and re-modelling of the tissue. Such metabolic control, however, has not been reported previously, so it is considered less likely than the simpler exposure explanation.

Figure 7 shows the average ratios of Ba/Sr, along with two standard deviation error bars, for all individuals and microstructure categories. Within the two Danish medieval and post-medieval towns, Ba/Sr-ratios vary greatly as can be seen by comparing Ribe's X1256/KLR-10810 and X1029/KLR-10831, and Viborg's X27/KLR-7292 and X1050/KLR-11500. Such variation indicative of differences in Ba and Sr exposure within the two towns is more likely attributable to the diet than the environmental setting. Danish towns at that time were rather small, and individuals could easily have moved throughout them during the course of their daily work. Environmental exposure to Ba and Sr within the confines of the town must have been about the same, so differences in Ba/Sr-ratios are more likely to stem from the food regularly consumed.

Finer details are partly lost in the logarithmic plots of the Sr-distributions in Fig. 6. In Fig. 8, however, the Sr distribution plots are shown for all six individuals on a linear scale. That provides a more detailed account of changes in diet or residential location that some individuals apparently experienced during their lives.

Turning first to the Apostle/KLR-11251, the laminar bone and 1st generation osteons are low in Sr, varying for the most part between 90 and 130 µg g^{-1} (Fig. 8b). The 3rd generation osteons show a different range of Sr concentration values, largely between 120 and 150 µg g^{-1}. The 2nd generation osteons are distributed between these extremes. Based on these results, it is possible that this individual moved from one geologically distinctive locale to another during the part of his life recorded by bone remodelling. The Sr concentrations tend to be low compared to the Danish skeletons, which may reflect differences in Sr availability between Denmark and land around the eastern Mediterranean.

In the individual from Maiori only 2nd and 3rd generation osteons are sampled (Fig. 8a). The distribution of the 2nd generation osteons peaks at a Sr concentration of 40 to 70 µg g^{-1}, but has a long tail extending past 300 µg g^{-1}. The 3rd generation osteons also extend up to 300 µg g^{-1}, but here the distribution is more uniform than in the 2nd generation osteons, with most values ranging from 60 to 150 µg g^{-1}.

In the medieval skeleton from Viborg Cathedral, X27/KLR-7292, the laminar bone is relatively low in Sr, between 175 and 325 µg g^{-1} (Fig. 8e). The 1st, 2nd, and 3rd generation osteons exhibit approximately the same Sr-concentration distributions, virtually all ranging from 200 to 500 µg g^{-1}. This pattern can be interpreted as an early move followed by a relatively stationary existence for the rest of that individual's life. In contrast, the post-medieval woman from Ribe designated X1029/KLR-10831 shows a gradual shift from 1st generation osteons, mostly between 50 and 350 µg g−1, to the 2nd and 3rd generation osteons that mostly range from about 100 to 700 µg g^{-1} (Fig. 8d). The 3rd generation osteons, however, have what appear to be a bimodal distribution. That change in the 3rd generation osteons is consistent with a move or change in diet, perhaps resulting from a

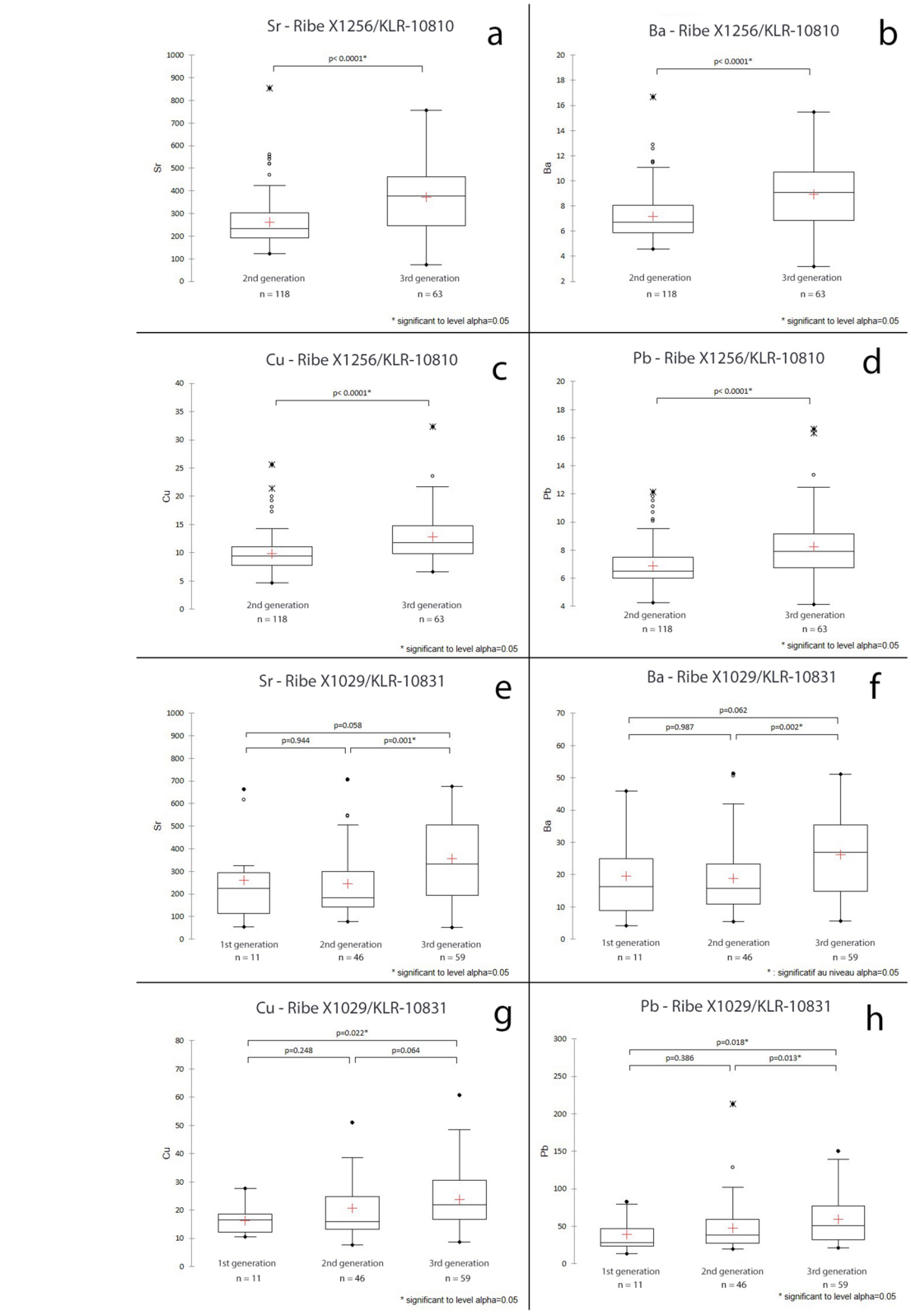
Sr - Ribe X1256/KLR-10810
a
p< 0.0001*
Sr
2nd generation
n = 118
3rd generation
n = 63
* significant to level alpha=0.05
Ba - Ribe X1256/KLR-10810
b
p< 0.0001*
Ba
2nd generation
n = 118
3rd generation
n = 63
* significant to level alpha=0.05
Cu - Ribe X1256/KLR-10810
c
p< 0.0001*
Cu
2nd generation
n = 118
3rd generation
n = 63
* significant to level alpha=0.05
Pb - Ribe X1256/KLR-10810
d
p< 0.0001*
Pb
2nd generation
n = 118
3rd generation
n = 63
* significant to level alpha=0.05
Sr - Ribe X1029/KLR-10831
e
p=0.058
p=0.944
p=0.001*
Sr
1st generation
n = 11
2nd generation
n = 46
3rd generation
n = 59
* significant to level alpha=0.05
Ba - Ribe X1029/KLR-10831
f
p=0.062
p=0.987
p=0.002*
Ba
1st generation
n = 11
2nd generation
n = 46
3rd generation
n = 59
* : significatif au niveau alpha=0.05
Cu - Ribe X1029/KLR-10831
g
p=0.022*
p=0.248
p=0.064
Cu
1st generation
n = 11
2nd generation
n = 46
3rd generation
n = 59
* significant to level alpha=0.05
Pb - Ribe X1029/KLR-10831
h
p=0.018*
p=0.386
p=0.013*
Pb
1st generation
n = 11
2nd generation
n = 46
3rd generation
n = 59
* significant to level alpha=0.05

(See figure on next page.)

Fig. 5 Boxplot of the distributions of the osteon chemistry of two archaeological interred individuals from Viborg Denmark, X27/KLR-7292 and X1050/KLR-11500, expressed as µg/g for each element. The p-values at the top of the diagram are Dunn's multiple comparison tests with alpha = 0.05 calculated after the one-way ANOVA analysis. The boxes indicate the extent between Q1 and Q3; the error bars indicate limits of Q1 + 1.5*IQR; the red crosses are the means; lines inside boxes are the medians; open circles are outliers in the range 1.5*IQR and 3 standard deviations; closed circles are outliers over 3 standard deviations from the mean; and crosses are extreme outliers according to the 3*IQR rule

shift in social status. A change in what this woman ate or where she lived might have been related to her showing visible signs of syphilis, as indicated by skeletal lesions. The woman from medieval Viborg's Sct. Morten cemetery, X1050/KLR-11500, shows a change in Sr-concentration distributions from one mostly centred around 100 µg g^{-1} in the 2nd generation osteons to the 3rd generation osteon values that mostly fall between ca. 150 to 250 µg g^{-1} (Fig. 8f). This shift might be indicative of an individual who moved at some point relatively late in life. For Maiori/KLR-11742 and Ribe X1256/KLR-10810, similar Sr distributions across the bone microstructure categories could indicate a relatively stationary existence, both in terms of residence and social status (Figs. 8a,c).

Cu and Pb relationship

Copper and Pb concentrations in individual osteons are also correlated with one other (Fig. 9). In general, the association between these two elements is not as strong as it is between Sr and Ba. Once again, the Apostle/KLR-11251 exhibits the lowest correlation between Cu and Pb. For one of the medieval individuals, Viborg's Sct. Morten X1050/KLR-11500, there seems to be two trendlines with different slopes, as indicated by dashed lines in Fig. 9f.

Figure 10 shows Pb/Cu ratios for the femoral samples, with the bone microstructure categories indicated. Within each person, Pb/Cu ratios are relatively similar across microstructure categories. There are, however, great differences among these individuals. That is even true for the pairs of skeletons from the two medieval and post-medieval Danish towns, Viborg and Ribe. The Apostle/KLR-11251 exhibits Pb/Cu ratios that are outliers insofar as they are much higher than what is seen in other samples. Figure 11 shows the Pb/Cu ratios versus the Ba/Sr ratios. The individuals are easily separable from one another when both ratios are plotted.

Discussion

Diagenesis

Much of the criticism in the 1980s concerning the use of elemental data for making inferences about past diets was based on analyses of crushed bone samples that ranged from grams to tens of milligrams. The anatomical specificity of the analysed material varied from quite general, such as simply "bone", to well-defined in terms of the specific bone sampled, and even the location and depth of the samples. The specific procedures used to obtain these samples was often unclear, even though Lambert et al. [47, 48] found that contamination by several elements, including Cu and Ba that are part of the present study, did not extend deeper than 400 µm into femoral cortical bone. These findings prompted Lambert et al. [47] to suggest that researchers remove a bone's outer surface before taking a sample for analysis. With regard to a shallow contamination of cortical bone by a number of elements, the findings of Lambert et al. [47, 48] were duplicated and refined by more recent studies [1, 2, 49, 50]. Furthermore, rather large differences in the trace-element chemistry of different bones have been observed, even within single individuals [8, 29, 51, 52]. The dismissal of Sr or Ba as having value in inferring dietary composition, therefore, is understandable in the context of what was known several decades ago.

For decades, both Fe and Mn concentrations in long-buried bone have been regarded as being heavily affected by diagenetic processes, so their study provides no information about the lives of past people. Nevertheless, Fe and Mn concentrations might tell us something if they should fall within a range consistent with no diagenetic effect, although what it might be is uncertain. As a step towards a more careful look at these elements, we present for the non-interred bones Fe concentrations for the microstructural categories ranging from 14.1 to 77.5 µg g^{-1} and for Mn from 2.04 to 6.62 µg g^{-1} (Table 1). It is possible that old bones that have never been buried might yield non-diagenetic results for these two elements. Much more work must be done before any possible utility of Fe and Mn in limited contexts can be established.

For the four elements of primary interest in this paper—Sr, Ba, Cu, and Pb—it is likely that postmortem alterations of bone chemistry were negligible. Sampled areas were located several hundred microns within the bone, well beyond the zones of possible surficial contamination previously identified in once-buried medieval Danish skeletal remains [1]. That is, the microstructural features examined were not located near bone surfaces that were directly exposed to the environment; for archaeologically derived bones, the surrounding soil. Furthermore, sampling sites avoided visually degraded areas or those with postmortem cracks, consistent with our lab's standard practice. Turning to the assessment of chemical

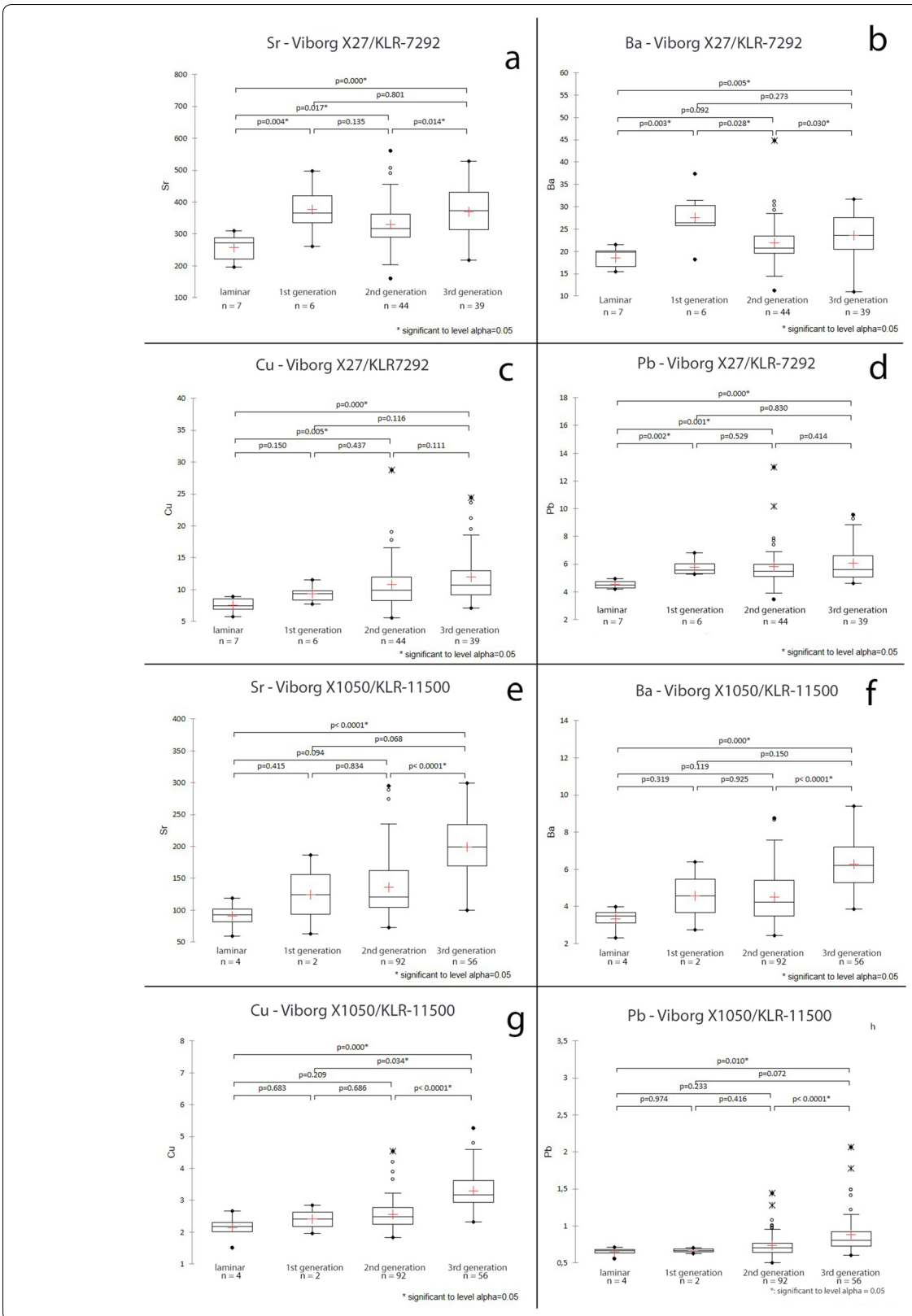
Sr - Viborg X27/KLR-7292
a
p=0.000*
p=0.801
p=0.017*
p=0.004*
p=0.135
p=0.014*
Sr
laminar n = 7
1st generation n = 6
2nd generation n = 44
3rd generation n = 39
* significant to level alpha=0.05
Ba - Viborg X27/KLR-7292
b
p=0.005*
p=0.273
p=0.092
p=0.003*
p=0.028*
p=0.030*
Ba
Laminar n = 7
1st generation n = 6
2nd generation n = 44
3rd generation n = 39
* significant to level alpha=0.05
Cu - Viborg X27/KLR7292
c
p=0.000*
p=0.116
p=0.005*
p=0.150
p=0.437
p=0.111
Cu
laminar n = 7
1st generation n = 6
2nd generation n = 44
3rd generation n = 39
* significant to level alpha=0.05
Pb - Viborg X27/KLR-7292
d
p=0.000*
p=0.830
p=0.001*
p=0.002*
p=0.529
p=0.414
Pb
laminar n = 7
1st generation n = 6
2nd generation n = 44
3rd generation n = 39
* significant to level alpha=0.05
Sr - Viborg X1050/KLR-11500
e
p< 0.0001*
p=0.068
p=0.094
p=0.415
p=0.834
p< 0.0001*
Sr
laminar n = 4
1st generation n = 2
2nd generatrion n = 92
3rd generation n = 56
* significant to level alpha=0.05
Ba - Viborg X1050/KLR-11500
f
p=0.000*
p=0.150
p=0.119
p=0.319
p=0.925
p< 0.0001*
Ba
laminar n = 4
1st generation n = 2
2nd generation n = 92
3rd generation n = 56
* significant to level alpha=0.05
Cu - Viborg X1050/KLR-11500
g
p=0.000*
p=0.034*
p=0.209
p=0.683
p=0.686
p< 0.0001*
Cu
laminar n = 4
1st generation n = 2
2nd generation n = 92
3rd generation n = 56
* significant to level alpha=0.05
Pb - Viborg X1050/KLR-11500
h
p=0.010*
p=0.072
p=0.233
p=0.974
p=0.416
p< 0.0001*
Pb
laminar n = 4
1st generation n = 2
2nd generation n = 92
3rd generation n = 56
*: significant to level alpha = 0.05

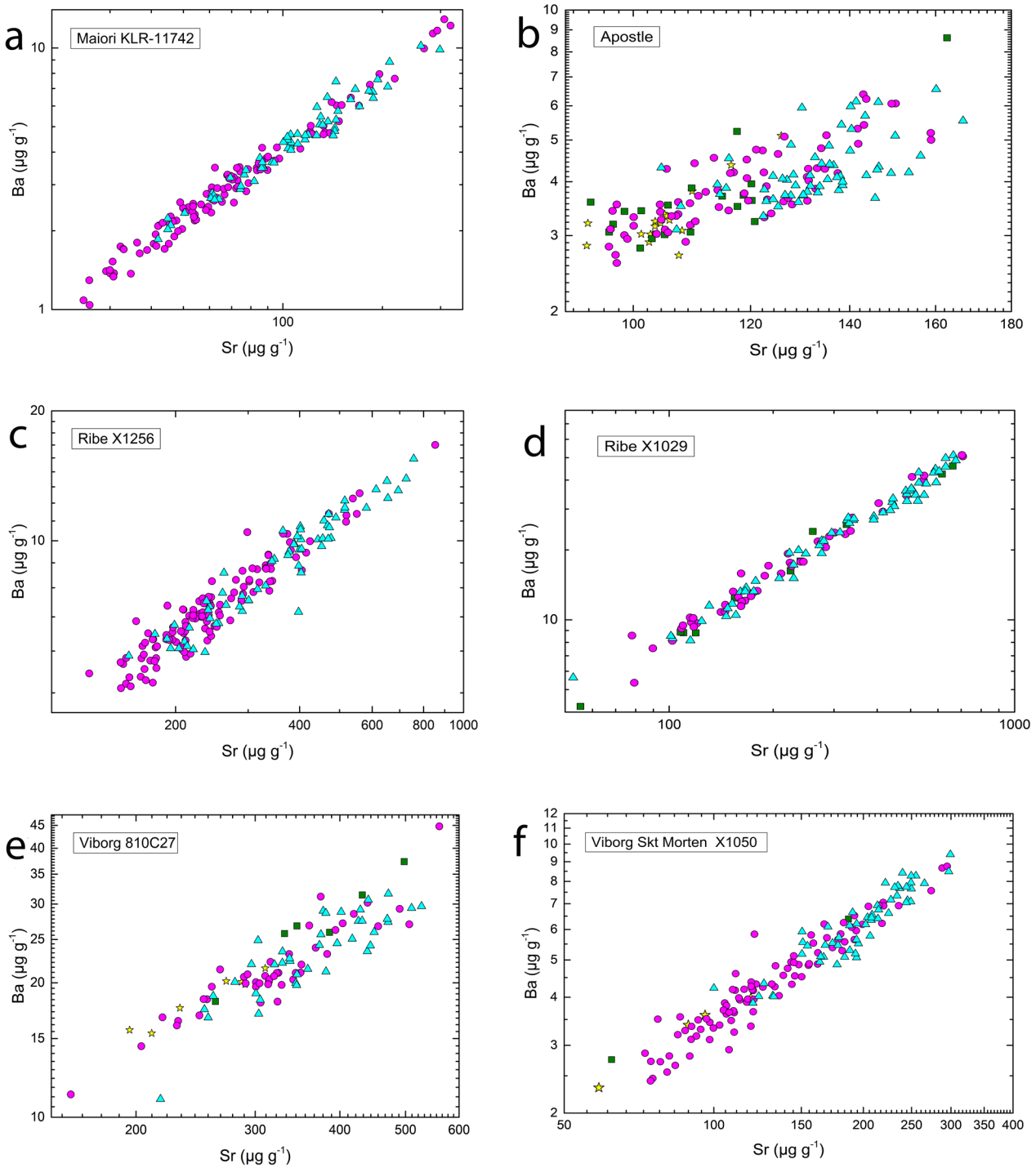

Fig. 6 Barium versus Sr concentrations, both in µg g^{-1}. Laminar bone, 1st, 2nd, and 3rd generation osteons are shown by yellow stars, dark green squares, magenta circles, and cyan triangles, respectively. Plots show: **a** a non-interred post-medieval middle aged male, Maiori/KLR-11742; **b** a non-interred ca. 2000 years old male, Apostle/KLR11251; **c** an interred 45–55 year old medieval to post-medieval male from Ribe in Denmark, X1256/KLR-10810; **d** an interred 37–47 year old post-medieval female from Ribe, X1029/KLR-10831; **e** an interred 24–30 year old medieval male from Viborg Cathedral in Denmark, X27/KLR-7292; and **f** an interred 21–23 year old medieval female from Viborg's Sct. Morten, X1050/KLR-11500

Table 2 Average Ba/Sr and Pb/Cu ratios, standard deviations of the ratios (SD), and r^2 values

KLR	Name	Field no.	Site	Sex	Age	Type	Ba/Sr	SD	r^2	Pb/Cu	SD	r^2
KLR-11951	Apostle	C94	Israel	M	45–55	laminar	0.0310	0.00388	0.7648	11.44	4.95	0.964
KLR-11951	Apostle	C94	Israel	M	45–55	1st gen	0.0331	0.00605	0.7304	15.03	7.68	0.174
KLR-11951	Apostle	C94	Israel	M	45–55	2nd gen	0.0331	0.00424	0.6623	16.57	6.46	0.248
KLR-11951	Apostle	C94	Israel	M	45–55	3rd gen	0.0324	0.00474	0.3042	18.77	10.1	0.0599
KLR-11742	Maiori	na	Maiori	M	Middle	laminar						
KLR-11742	Maiori	na	Maiori	M	Middle	1st gen						
KLR-11742	Maiori	na	Maiori	M	Middle	2nd gen	0.0432	0.00448	0.9829	1.137	0.285	0.748
KLR-11742	Maiori	na	Maiori	M	Middle	3rd gen	0.0407	0.00411	0.9392	1.257	0.324	0.554
KLR-10810	K1256	K1256	Ribe	M	45–55	laminar						
KLR-10810	K1256	K1256	Ribe	M	45–55	1st gen						
KLR-10810	K1256	K1256	Ribe	M	45–55	2nd gen	0.0286	0.00383	0.9125	0.724	0.127	0.689
KLR-10810	K1256	K1256	Ribe	M	45–55	3rd gen	0.0254	0.00434	0.9206	0.664	0.113	0.716
KLR-10831	K1029	K1029	Ribe	F	37–47	laminar						
KLR-10831	K1029	K1029	Ribe	F	37–47	1st gen	0.0771	0.00633	0.9846	2.260	0.777	0.759
KLR-10831	K1029	K1029	Ribe	F	37–47	2nd gen	0.0789	0.00767	0.9875	2.240	0.709	0.407
KLR-10831	K1029	K1029	Ribe	F	37–47	3rd gen	0.0755	0.00718	0.9743	2.513	0.803	0.507
KLR-7292	Viborg	810C 27A	Viborg	M	24–30	laminar	0.0730	0.00378	0.9534	0.611	0.0947	0.00600
KLR-7292	Viborg	810C 27A	Viborg	M	24–30	1st gen	0.0732	0.00397	0.9434	0.626	0.0777	0.189
KLR-7292	Viborg	810C 27A	Viborg	M	24–30	2nd gen	0.0671	0.00637	0.8076	0.573	0.153	0.725
KLR-7292	Viborg	810C 27A	Viborg	M	24–30	3rd gen	0.0642	0.00710	0.7209	0.532	0.118	0.610
KLR-11500	Viborg	X1050	Viborg	F	21–23	laminar	0.0372	0.00227	0.9636	0.312	0.0381	0.983
KLR-11500	Viborg	X1050	Viborg	F	21–24	1st gen	0.0392	0.00498	1.0000	0.284	0.0362	1.000
KLR-11500	Viborg	X1050	Viborg	F	21–25	2nd gen	0.0338	0.00347	0.9266	0.287	0.0336	0.651
KLR-11500	Viborg	X1050	Viborg	F	21–26	3rd gen	0.0317	0.00293	0.8632	0.267	0.0489	0.586

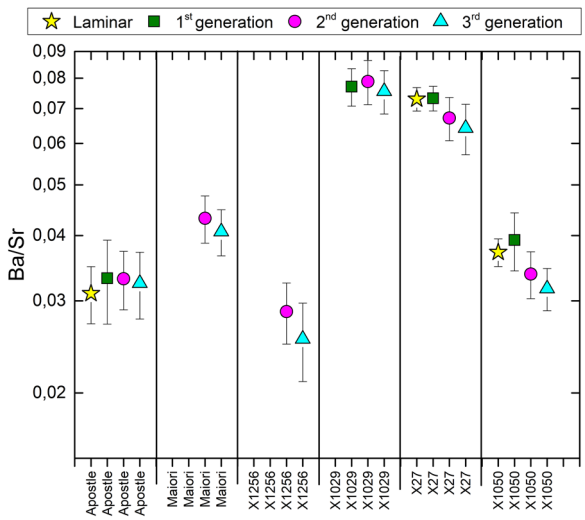

Fig. 7 Ba/Sr-ratios calculated for each microstructure category in each of the six individuals: means of Ba/Sr-ratios and error bars of two standard deviations of the mean ratios are shown

composition, individual microstructural elements, mostly complete or fragmentary osteons, were targeted for sampling. Openings in the bone, notably Haversian canals, where foreign material might be found were also avoided in the present data set. Foreign material in such openings was shown to be a contaminant in one archaeological skeleton reported in Rasmussen et al. [1]. Finally, cross-sectional images produced in this study, such as shown in Fig. 1 and in earlier work that includes a modern (never buried) bone along with archaeological specimens [1], show uneven element distributions across osteons. Notably that includes a contrast between osteon lamellae and cement lines in skeletons that were never interred in the ground as well as archaeological bones buried in soil for centuries. An uneven trace element distribution in old and recent bones in this study is consistent with what other researchers have reported for modern bones [5, 6]. Taken together, these findings increase confidence that results largely free from the effects of diagenesis are possible with archaeological specimens, as long as proper precautions are followed as outlined in a study that specifically addressed that issue [1].

Previous work has shown that there is an explicable pattern in Cu and Pb concentrations in bulk bone samples

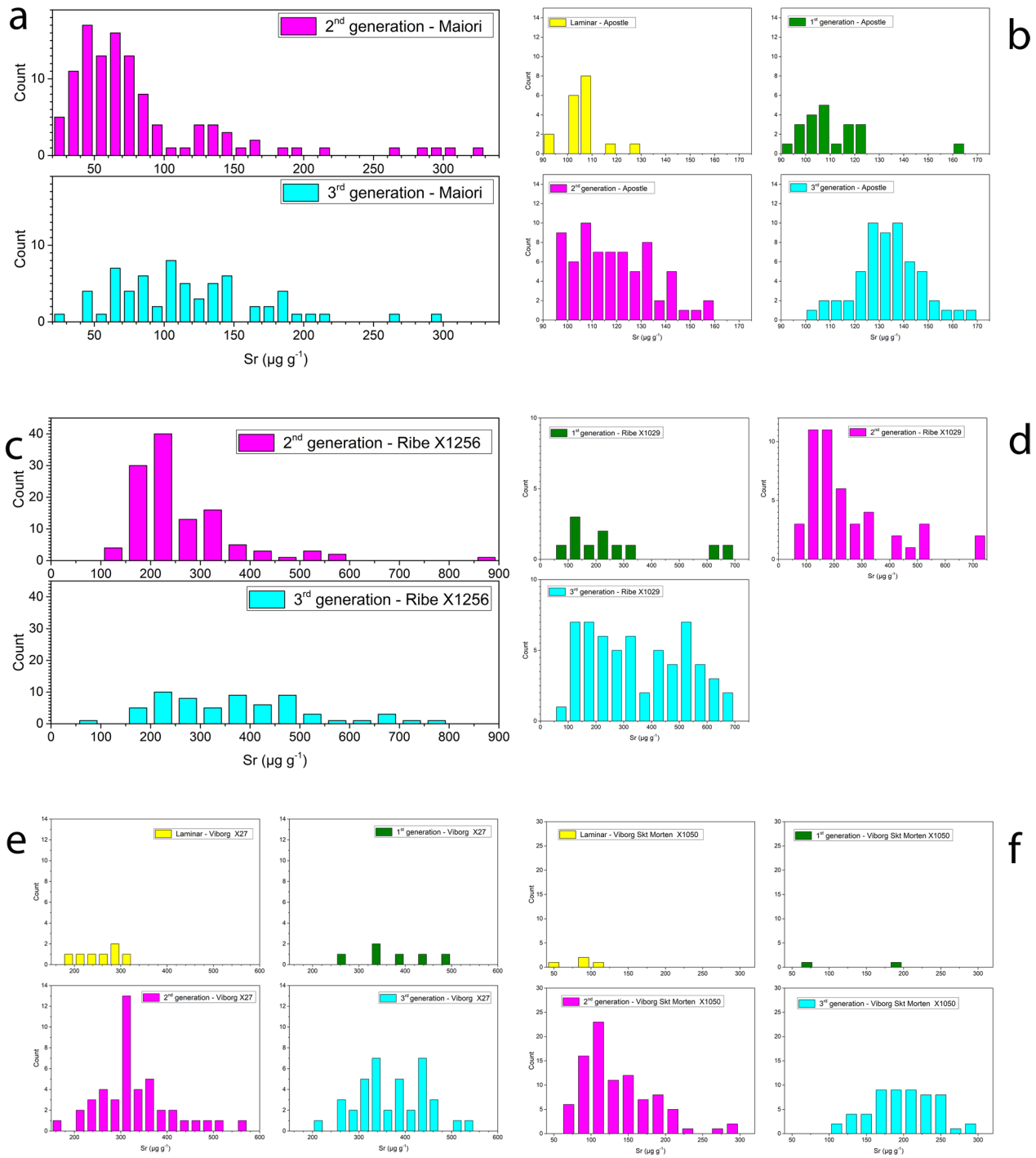

Fig. 8 Detailed Sr-distributions for all samples and all bone microstructure categories. Plots show: **a** a non-interred post-medieval middle aged male, Maiori/KLR-11742; **b** a non-interred *ca.* 2000 years old male, Apostle/KLR11251; **c** an interred 45–55 year old medieval to post-medieval male from Ribe in Denmark, X1256/KLR-10810; **d** an interred 37–47 year old post-medieval female from Ribe, X1029/KLR-10831; **e** an interred 24–30 year old medieval male from Viborg Cathedral in Denmark, X27/KLR-7292; and **f** an interred 21–23 year old medieval female from Viborg's Sct. Morten, X1050/KLR-11500

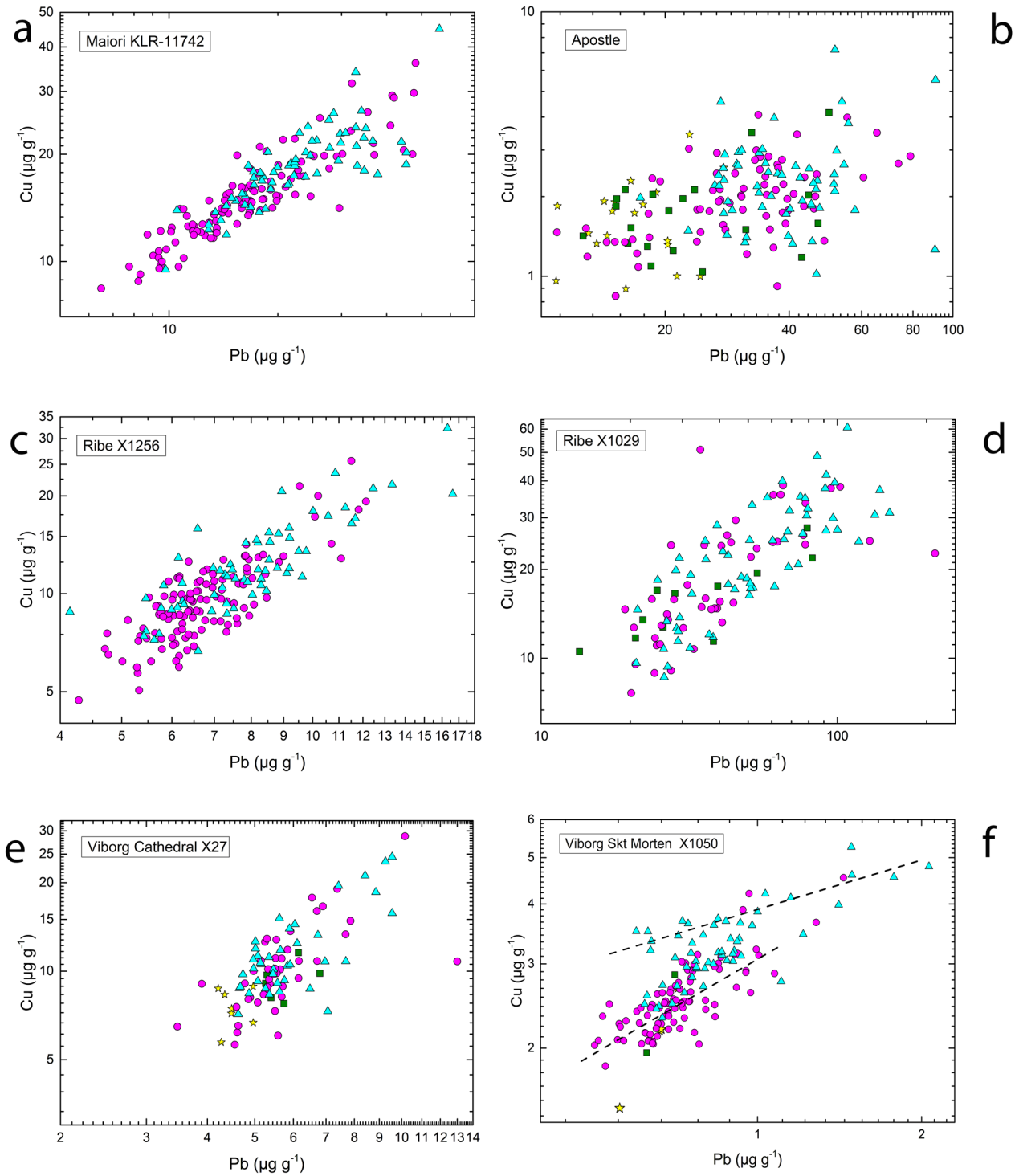

Fig. 9 Copper versus Pb concentrations, both in µg g^{-1}. Laminar bone, 1st, 2nd, and 3rd generation osteons are shown by yellow stars, dark green squares, magenta circles, and cyan triangles, respectively. The plot layout is the same as in Fig. 6. Plots show: **a** a non-interred post-medieval middle aged male, Maiori/KLR-11742; **b** a non-interred *ca.* 2000 years old male, Apostle/KLR11251; **c** an interred 45–55 year old medieval to post-medieval male from Ribe in Denmark, X1256/KLR-10810; **d** an interred 37–47 year old post-medieval female from Ribe, X1029/KLR-10831; **e** an interred 24–30 year old medieval male from Viborg Cathedral, X27/KLR-7292; and **f** an interred 21–23 year old medieval female from Viborg's Sct. Morten, X1050/KLR-11500

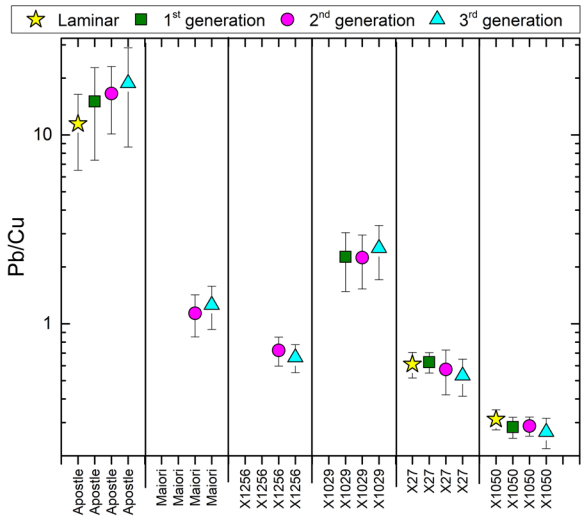

Fig. 10 Pb/Cu-ratios calculated for each microstructure category in the six individuals: average ratio and error bars of 2 standard deviations of the mean are shown

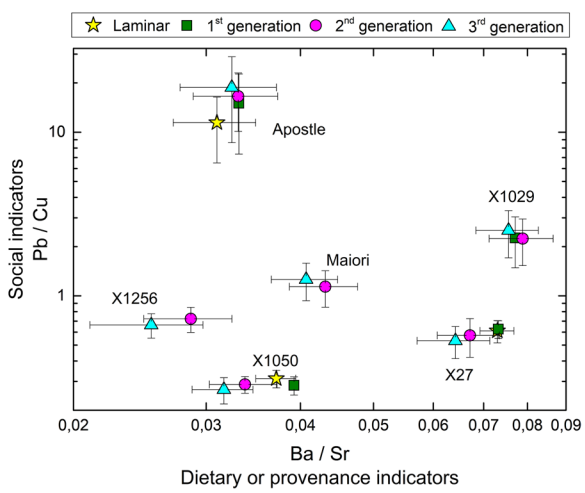

Fig. 11 Pb/Cu-ratios versus Ba/Sr-ratios. Laminar bone, 1st, 2nd, and 3rd generation osteons are shown by yellow stars, dark green squares, magenta circles, and cyan triangles, respectively. The femoral samples are from a centuries old, non-interred Italian, Maiori/KLR-11742; a ca. 2000 years old person, Apostle/KLR11251; two excavated skeletons from Ribe, X1256/KLR-10810 and X1029/KLR-10831; and skeletons from Viborg's Cathedral, X27/KLR-7292, and its Sct. Morten cemetery, X1050/KLR-11500

from medieval to post-medieval skeletons interred in cemeteries in Denmark and northern Germany [37, 52]. The distribution of these elements among the different bone microstructural elements is perhaps the strongest reason to believe a biogenetic signal is retained that is not masked by diagenetic processes [1]. That is, Cu and Pb concentrations vary across the sampled areas, with differences in trace element content conforming precisely to microstructural features, notably intact or fragmentary osteons. Furthermore, in the four medieval skeletons, the covariation in Cu and Pb concentrations in microstructural features is consistent with a much larger and diverse array of bulk bone samples that show similar patterning among individuals from different locations and socioeconomic strata in medieval Denmark [37]. In other words, Cu and Pb concentration values varied among individual osteons as predicted from analyses of bone samples that lacked specificity down to the microstructural level.

A strong positive correlation between Sr and Ba is likewise an argument against diagenesis having had a major effect on the concentrations of these two elements. Of these two elements, Ba is the more likely to be affected by diagenesis [1, 37, 48]. Microstructure sampling, however, yields a close association between Sr and Ba in both long-buried skeletons from different cemeteries and the remains of individuals that had never been buried. If Ba had a diagenetic origin—more precisely, if the effects of diagenesis masked a biogenic signal—it is unlikely that such a clear and consistent pattern would have been apparent regardless of the postmortem histories of the skeletal material.

Examining the chemical composition of bone microstructure, down to the level of features formed at different times during an individual's life, takes us a step closer to ensuring that the results represent a true signal, not a postmortem alteration of the bone's original composition. That has practical implications for the use of bone chemistry to address archaeological research questions. In fact, the results of the present work are broadly consistent with those of Scharlotta and colleagues [53] who also point out the advantages of examining individual osteons rather than relying on bulk bones samples.

Bulk sampling procedures, of course, can avoid surface degradation by focusing on the interior of cortical bone. But the later infilling of openings formed during life, such as Haversian canals, or those that developed after death through cracking or microbial invasion remains a problem. Nevertheless, bulk sampling has one clear advantage over the procedure outlined in this paper. It is far easier and cheaper than detailed characterizations of cortical bone microstructure visible in cross-sections. It is, therefore, important to determine what can, and cannot, be learned from bulk sampling. The results of the present work are encouraging in that regard, at least for northern European skeletons that are only up to a thousand years old, as discussed above for Cu and Pb where the analysis of microstructural details is consistent with previous results from bulk samples.

Strontium and Ba as dietary indicators

Strontium and Ba have been widely used as dietary and provenance indicators [8, 25, 33, 35–37, 54–57]. The use of Sr and Ba concentrations for making inferences about diet was largely abandoned in the late 1980s, being replaced almost entirely by analyses of Sr isotopes. Recently, however, there has been a revival of interest in elemental analyses following the recognition that they provide information about life in the past that differs, but complements, what can be learned from isotopic data [1, 25, 33–37, 53, 57].

Concentrations of Sr and Ba in bone can vary through an individual's life for two reasons of concern here. First, the person might have migrated from one geographical location to another, which would be visible if the two locations had different levels of bioavailable Sr and Ba in surface water and food that were attributable to the geological context. Second, a major change could have taken place in what a person ate, such as a shift from a mainly meat to a largely plant-based diet. Differences in Sr and Ba between different types of modern food are well documented [58, 59]. However, precisely how Sr and Ba concentrations in food translate into skeletal Sr and Ba concentrations is still incompletely understood [60].

Alterations can be expected in skeletal trace-element chemistry when dietary composition changed dramatically. For example, if the food consumed shifted from predominantly meat to grain products, the amount of Sr and Ba ingested would increase greatly. Such a change in the diet would perhaps result in several times greater for Ba and several tens of times higher for Sr [58, 59].

Changes in Sr and Ba bone concentrations could have come about because a person migrated from one place to another. While the availability of different kinds of food might not have been the same before and after a move, in most instances the change in geological setting was more likely to have had a measurable effect on the elemental composition of the migrant's skeleton. That is because centuries or millennia ago the food consumed was largely, if not entirely, produced locally. The homogenizing effects of food regularly obtained from distant places, to the extent it actually occurs, had to wait until the development of regular and effective transportation and distribution systems for bulk commodities.

The emphasis placed here on the geological setting is not meant to minimize the dietary variation that existed within communities. Especially in socially stratified societies such as those of medieval Europe, dietary composition might have changed as an individual gained, or lost, wealth and social status. That would occur even if the person continued to reside in the same community. Some variation can also be expected within particular socioeconomic groups in stratified societies. It could have come about through personal preferences that influenced dietary choices, as well as differences in household access to food because of local, including seasonal, circumstances. Variation in diets might also have arisen from cultural prescriptions regarding what was appropriate for people of different age and sex groups to eat, as well as what was fed to people who had fallen ill. For these reasons, and others as well, Sr and Ba concentrations are best interpreted through the use of large and diverse samples of skeletons from well-documented archaeological contexts [37]. Analysing skeletons that happen to be available and characterizing them in general terms rather than delving into the specific nature of the communities from which they were drawn will not provide culturally meaningful results.

Copper and Pb as socioeconomic indicators

Copper has been used as a palaeodietary indicator [8, 61, 62], but the relationship between its presence in food, uptake in the gastrointestinal tract, and subsequent deposition in bones is unclear [63–65]. High concentrations of Cu have been detected in archaeological remains from individuals thought to have been involved in mining Cu or manufacturing objects from it [51, 66, 67]. In medieval and post-medieval Danish populations, much of the variation in Cu exposure was likely to have been related to objects made of the element or its alloys encountered in everyday life, perhaps most notably kitchen utensils [37]. In fact, Cu concentrations in Danish skeletal remains track rather nicely residence location, specifically rural villages versus towns. Residence location was related to access to metal containers used when cooking and storing food that, in turn, was linked to trade networks centred on regional market towns. For some townsfolk, a high socioeconomic status meant they possessed the means to obtain relatively rare and valued items, including utilitarian household goods. Although Cu exposure can be indicative of high social status, the picture could be clouded by special circumstances, such as work in a coppersmith's workshop or living near one. Servants working within wealthy households would also have been exposed to Cu, much like their masters. As always, inferences from skeletons about past ways of life cannot be made without detailed knowledge of the local cultural context. It is here where population-level inferences should accommodate the details of individual life histories.

The significance of Pb in human and non-human skeletal remains from archaeological contexts is well established [39, 40, 52, 70–74]. Lead has received attention largely because of its known toxic effects and concentration in bone [68, 69]. Studies of archaeological bones have detected environmental pollution linked to urbanization,

and they have identified its association with social position. In medieval and early modern northern Europe, concentrations of Pb were likely to have been heavily influenced by exposure to lead-glazed ceramics, as well as waterpipes, roofs, and objects such as household utensils made partly or entirely of Pb.

In a previous study of bulk samples taken from skeletons excavated from several Danish and northern German medieval cemeteries, an explicable pattern was found when Cu and Pb concentrations were plotted against one another [37]. A large sample, diverse archaeological contexts, and consistent results all pointed toward the two elements being associated with one another. The present work on bone chemistry at a microscopic level constitutes strong support for, and increases confidence in, those earlier findings.

Mobility and diet

As mentioned above, mobility and diet are inextricably related to one another in past populations, including those of the medieval and early modern periods. For single individuals, such as those examined here, it is likely that major shifts in the trace-element composition of bone during the course of a lifetime were often related to movement from one place to another. That is because the food and liquid consumed would have largely come from local sources, even if the range and quantities of what was ingested remained the same before and after the individual moved.

Turning to the medieval Danes with all four microstructure categories, it is likely they moved during their lifetimes. The concentrations of Sr and Ba in the laminar bone of the person from Viborg Cathedral, X27/KLR-7292, were different from those in the 1st, 2nd, and 3rd generation osteons, which were higher (Figs. 5, 6). When he was young, this man perhaps lived in one place, but spent much of his life elsewhere. If indeed he lived in the same place, presumably Viborg, for much of his life, then the overall increase in Pb and Cu in the three osteon categories could indicate increasing social status over time. That would make sense if he became more prosperous as he got older. If such an interpretation is correct, then it follows that the woman from Viborg's Sct. Morten cemetery, X1050/KLR-11500, experienced at least one such change in her life, as indicated by the Sr and Ba values in the 2nd and 3rd generation osteons (Figs. 5, 6). Here too the Pb and Cu values tell much the same story. The sample of laminar bone and 1st generation osteons is too small to do more than suggest she experienced as many as two elementally identifiable changes in her life. Two individuals, of course, are too few to serve as the basis of any definitive conclusions about life in the past. That said, examinations of more individuals from contexts with good contextual controls can establish whether major shifts in trace element exposure during a lifetime were common or not, and if increases in social position through the most productive years of life were characteristic of some times and places, but not others.

The skeletal sample is far too small and potentially biased to reach any solid conclusions about Danish life a half-millennium ago. The results are intriguing, however, because the medieval Viborg skeletons indicate that occasional movement from one place to another might have been greater than commonly thought, at least for the residents of regionally important towns. A much larger and more representative sample of Danish communities at that time, and the social variation within them, is needed to assess the mobility of various segments of medieval society.

Turning to the Apostle/KLR-11251 femur, it appears that St. James the Lesser (if it is really him) moved from one place to another during the part of his life recorded by the sampled complete and fragmentary osteons (Fig. 3). That is true of all four of the principal elements examined here. This finding is of interest because little is known about his life. Of the individuals investigated in this study, the Apostle had the weakest correlation between Cu and Pb. Whatever the sources of Cu and Pb exposure might have been, they were not as tightly associated in his lifetime as they were for people in medieval to post-medieval times. Once again, larger samples are needed before reaching any conclusions, although the bone microstructure findings are sufficient to highlight the potential for this line of work.

Microstructure versus bulk sampling

As might be expected from an uneven distribution of trace elements in cortical bone, the elemental composition of individual osteons often will not conform to bulk-sample findings. The latter are composed of many different osteons, each with a different chemical signature. Bulk sample results are useful insofar as they provide an indication of trace element exposure across many years of life, the duration of which is unknown in any sampled individual. Bone turnover in adults, the speed of which varies by age, is sufficiently slow in the inorganic fraction of bone that it captures a biogenetic signal that might span well over a decade [75–77]. Chemical signals from bulk samples and multiple separately sampled osteons are not necessarily the same, as shown by an isotopic study of the organic fraction of centuries old bones [7]. Although much remains to be learned about what can be gained from sampling individual microstructural features, doing so has the potential of providing more fine-grained and informative chemical life histories [7].

Improvements in our ability to document chemical life histories are especially noteworthy in situations where there is a reason to be interested in what happened to a specific person. One example is the Apostle St James the Lesser. There is also the very real possibility that individual life histories, in combination, can illuminate what took place in entire communities. Although the potential for such work exists [1, 53], there remains the challenge of scaling it upwards so that general trends in community formation and composition can be identified.

One component of future work would be to evaluate the microstructure classification scheme introduced here with other elements and isotopes. With regard to the latter, one way to proceed is to follow the lead of Koons and Tuross [7] with the organic fraction of bone. What is likely to be especially useful is a combination of trace elements and light stable isotopes.

Another concern is establishing the proper cultural context for the skeletons that are examined. That is especially important because the time and expense involved in the chemical characterization of bone microstructure means that the number of individuals sampled, for the most part, will likely be small. The medieval Danes in this pilot study highlight that issue. The periodic moves in people's lives implied by our findings might, or might not, have been characteristic of the society as a whole. Perhaps such mobility was true of only a narrow slice of Danish society: the inhabitants of towns, and maybe even particular segments of those communities. Fortunately, that issue can be addressed in this instance by looking at skeletons from multiple archaeologically well-characterized cemeteries within towns and those associated with outlying villages. In short, the process of reconstructing life experiences from archaeological skeletons might start with bone chemistry, but much more is required to make reasonable inferences about the past.

Conclusions

Cortical bone cross-sections from two femora that had never been buried—one dating to the eighteenth or nineteenth centuries, and another ca. 2000 years old—were subjected to LA-ICP-MS analyses, as were four femora excavated from Danish medieval to post-medieval cemeteries. The diverse array of specimens shows that the chemical composition of bone microstructure can be mapped and used to interpret various aspects of individual lives. Diet, residence location, and social status can be identified using the four principal elements examined here: Sr, Ba, Cu, and Pb.

Four bone microstructure categories defined in this study provide a temporal perspective on the elemental composition of bone formed at different times during the lives of six people. While much can be learned from specific individuals, the real benefit, and challenge, posed by mapping trace element distributions in cross-sections of cortical bone will come when large samples of contextually well-characterized skeletons are analysed. Doing so has the potential of contributing to our understanding of how communities in the past were structured, as well as the movement of people among them. Although such analyses are time-consuming, hence more expensive than those based on bulk bone samples, the return in terms of information gained has the potential of far outweighing the additional cost involved.

Supplementary information

Supplementary information accompanies this paper at https://doi.org/10.1186/s40494-020-00457-1.

Additional file 1. The concentrations of Sr, Ba, Cu, and Pb for each of the scored structures, laminar bone, 1st, 2nd, or 3rd generation osteons, as well as their coordinates in the cross-sections analyzed.

Additional file 2. Spearman correlation matrix.

Additional file 3. Means, relative standard deviations, and relative standard deviations (RSD) for each bone microstructure category for each individual.

Abbreviations

ANOVA: Analysis of variance; ICP-MS: Inductively coupled plasma mass spectrometry; LA-ICP-MS: Laser ablation inductively coupled plasma mass spectrometry; LOD: Limit of detection; LOQ: Limit of quantification; PCA: Principal component analysis; RSD: Relative standard deviation; SD: Standard deviation; SR: Synchrotron radiation.

Acknowledgements

We are grateful for permissions to sample skeletons from Ribe given by Morten Søvsø. Dorthe Dangvard Pedersen and Vicki R.L. Kristensen helped collect skeletal data. Pia Klingenberg Haussmann is thanked for her help in the laboratory and in collecting samples. Brother Agnello Stoia, parish priest of the Church of the Twelve Holy Apostles in Rome, is thanked for permission to sample the relics of Apostle St James the Lesser and for support throughout the project. The lord major of Maiori, Antonio Capone, is thanked for permissions and help with the fieldwork. Financial support by VELUX Fonden, the EU Interreg Office, and Det Frie Forskningsråd are gratefully acknowledged. Comments from anonymous reviewers greatly improved the manuscript.

Authors' contributions

Conceived and designed the experiments: KLR. Performed the chemical analyses: KLR and LS. Analysed the data: KLR, LS, TD, and GRM. Contributed as leading field archaeologists and with historical references SS, MT, and LAL. Contributed to the anthropological and laboratory components of the work, including the interpretation of results and acquisition of references: KLR, TD, GRM, JLB, NL, JLT, SS, and MT. Wrote the paper, with comments from other participants: KLR, GM, and TD. All authors read and approved the final manuscript.

Funding

The present work has been funded by EU Interreg Office for financial support to the project Bones4Culture (10/13122). The Velux Fonden (VELUX 32089); Det Frie Forskningsråd (DFF-6107-00284).

Availability of data and materials

Data are available upon request from the authors.

Ethics approval and consent to participate
No ethical issues.

Competing interests
We declare there are no potential competing interests.

Author details
[1] Cultural Heritage and Archaeometric Research Team (CHART), Department of Physics, Chemistry and Pharmacy, University of Southern Denmark, Campusvej 55, 5230 Odense M, Denmark. [2] Department of Anthropology, Pennsylvania State University, University Park, PA 16802, USA. [3] Laboratory of Biological Anthropology, Institute of Forensic Medicine, University of Copenhagen, Blegdamsvej 3, 2200 Copenhagen, Denmark. [4] Institute of Forensic Medicine, University of Southern Denmark, J. B. Winsløws Vej 17, 5000 Odense C, Denmark. [5] Pontifical Institute of Christian Archaeology, Via Napoleone III, 1, 00185 Roma, Italy. [6] Laboratory of Science and Techniques Applied to Archaeology, University Suor Orsola Benincasa, Via Santa Caterina da Siena, 37, 80135 Naples, Italy. [7] Viborg Museum, Hjultorvet 4, 8800 Viborg, Denmark. [8] Section of Anthropology (ADBOU), Department of Forensic Medicine, University of Southern Denmark, Campusvej 55, 5230 Odense, Denmark.

Received: 8 June 2020 Accepted: 28 October 2020
Published online: 07 November 2020

References

1. Rasmussen KL, Milner GR, Skytte L, Lynnerup N, Thomsen JL, Boldsen JL. Mapping diagenesis in archaeological human bones. Herit Sci. 2019;7:41.
2. Swanston T, Varney T, Coulthard I, Feng R, Bewer B, Murphy R, et al. Element localization in archaeological bone using synchrotron radiation X-ray fluorescence: identification of biogenic uptake. J Archaeol Sci. 2012;39:2409–13.
3. Swanston T, Varney TL, Kozachuk M, Choudhury S, Bewer B, Coulthard I, et al. Franklin expedition lead exposure: new insights from high resolution confocal X-ray fluorescence imaging of skeletal microstructure. PLoS ONE. 2018;13:e0202983.
4. Choudhury S, Swanston T, Varney TL, Cooper DML, George GN, Pickering IJ, et al. Confocal X-ray fluorescence imaging facilitates high-resolution elemental mapping in fragile archaeological bone. Archaeometry. 2016;58:207–17.
5. Pemmer B, Roschger A, Wastl A, Hofstaetter JG, Wobrauschek P, Simon R, et al. Spatial distribution of the trace elements zinc, strontium and lead in human bone tissue. Bone. 2013;57:184–93.
6. Wittig NK, Palle J, Østergaard M, Frølich S, Birkbak ME, Spiers KM, et al. Bone biomineral properties vary across human osteonal bone. ACS Nano. 2019;13:12949–56.
7. Koon H, Tuross N. The Dutch whalers: a test of a human migration in the oxygen, carbon and nitrogen isotopes of cortical bone collagen. World Archaeol. 2013;45:360–72.
8. Buikstra JE, Frankenberg S, Lambert JB, Xue L. Multiple elements: multiple expectations. In: Price TD, editor. The chemistry of prehistoric human bone. Cambridge: Cambridge University Press; 1989. p. 155–210.
9. Skytte L, Rasmussen KL. Sampling strategy and analysis of trace element concentrations by inductively coupled plasma mass spectroscopy on medieval human bones—the concept of chemical life history. Rapid Com Mass Spec. 2013;27:1591–9.
10. Williams AMM, Siegele R. Iron deposition in modern and archaeological teeth. Nucl Instrum Meth B. 2014;335:19–23.
11. Hadjidakis DJ, Androulakis II. Bone remodeling. Ann NY Acad Sci. 2006;1092:385–96.
12. Morgan EF, Barnes GL, Einhorn TA. The bone organ system: form and function. In: Marcus R, Feldman D, Dempster DW, Luckey M, Cauley JA, editors. Osteoporosis. 4th ed. Amsterdam: Academic Press; 2013. p. 3–20.
13. Britz HM, Thomas CDL, Clement JG, Cooper DML. The relation of femoral osteon geometry to age, sex, height and weight. Bone. 2009;45:77–83.
14. Gocha TP, Robling AG, Stout SD. Histomorphometry of human cortical bone: applications to age estimation. In: Katzenberg AM, Grauer AL, editors. Biological anthropology of the human skeleton. 3rd ed. Hoboken: Wiley-Blackwell; 2019. p. 145–88.
15. Stout SD, Paine RR. Brief communication: histological age estimation using rib and clavicle. Am J Phys Anthropol. 1992;87:111–5.
16. Lynnerup N, Frohlich B, Thomsen JL. Assessment of age at death by microscopy: unbiased quantification of secondary osteons in femoral cross sections. Forensic Sci Int. 2006;159S:S100–3.
17. Keough N, L'Abbé EN, Steyn M. The evaluation of age-related histomorphometric variables in a cadaver sample of lower socioeconomic status: implications for estimating age at death. Forensic Sci Int. 2009;191:114.e1-114.e6.
18. Goliath JR, Stewart MC, Stout SD. Variation in osteon histomorphometrics and their impact on age-at-death estimation in older individuals. Forensic Sci Int. 2016;262:282.e1-282.e6.
19. Maggio A, Franklin D. Histomorphometric age estimation from the femoral cortex: a test of three methods in an Australian population. Forensic Sci Int. 2019;303:109950.
20. Kristensen HK, Poulsen B. Danmarks byer i middelalderen. Aarhus: Aarhus Universitetsforlag; 2016.
21. Kulturhistorisk leksikon for Nordisk Middelalder. Nørhaven Bogtrykkeri A/S Viborg. 1981;6(147):150.
22. Price TD, Schoeninger MJ, Armelagos GJ. Bone chemistry and past behaviour: an overview. J Hum Evol. 1985;14:419–47.
23. Price TD, Blitz J, Burton J, Ezzo JA. Diagenesis in prehistoric bone: problems and solutions. J Archaeol Sci. 1992;19:513–29.
24. Vuorinen HS, Pihlman S, Mussalo-Rauhamaa H, Tapper U, Varrela T. Trace and heavy metal analyses of a skeletal population representing the town people in Turku (Åbo), Finland in the 16th-17th centuries: with special reference to gender, age and social background. Sci Tot Environ. 1996;177:145–60.
25. Burton JH, Price TD. The use and abuse of trace elements for paleodietary research. In: Ambrose SH, Katzenberg MA, editors. Biogeochemical approaches to paleodietary analysis. New York: Kluwer Academic; 2002. p. 159–71.
26. Fabig A, Herrmann B. Trace elements in buried human bones: intrapopulation variability of Sr/Ca and Ba/Ca ratios—diet or diagenesis? Naturwissenchaften. 2002;89:115–9.
27. Reiche I, Favre-Quattropani L, Vignaud C, Bocherens H, Charlet L, Menu M. A multi-analytical study of bone diagenesis: the Neolithic site of Bercy (Paris, France). Meas Sci Technol. 2003;14:1608–19.
28. Trueman CNG, Behrensmeyer AK, Tuross N, Weiner S. Mineralogical and compositional changes in bones exposed on soil surfaces in Amboseli National Park, Kenya: diagenetic mechanisms and the role of sediment pore fluids. J Archaeol Sci. 2004;31:721–39.
29. Rasmussen KL, Skytte L, Pilekær C, Lauritsen A, Boldsen JL, Leth PM, et al. The distribution of mercury and other trace elements in the bones of two human individuals from medieval Denmark—the chemical life history hypothesis. Heritage Sci. 2013;1:10.
30. Keenan SW. From bone to fossil: a review of the diagenesis of bioapatite. Am Mineral. 2016;101:1943–51.
31. López-Costas O, Lantes-Suárez O, Cortizas AM. Chemical compositional changes in archaeological human bones due to diagenesis: type of bone vs soil environment. J Archaeol Sci. 2016;67:43–51.
32. Kendall C, Eriksen AMH, Kontopoulos I, Collins MJ, Turner-Walker G. Diagenesis of archaeological bone and tooth. Palaeogeogr Palaeoclimatol Palaeoecol. 2018;491:21–37.
33. Schutkowski H, Herrmann B, Wiedemann F, Bocherens H, Grupe G. Diet, status and decomposition at Weingarten: trace element and isotope analyses on early mediaeval skeletal material. J Archaeol Sci. 1999;26:675–85.
34. Mays S. Bone strontium: calcium ratios and duration of breastfeeding in a mediaeval skeletal population. J Archaeol Sci. 2003;30:731–41.
35. Torino M, Boldsen JL, Tarp P, Rasmussen KL, Skytte L, Nielsen L, et al. Convento di San Francesco a Folloni: the function of a medieval Franciscan friary seen through the burials. Heritage Sci. 2015;3:27.
36. Lösch S, Moghaddam N, Grossschmidt K, Risser DU, Kanz F. Stable isotope and trace element studies on gladiators and contemporary Romans from Ephesus (Turkey, 2nd and 3rd Ct AD)—implications for differences in diet. PLoS ONE. 2014;9:e110489.
37. Rasmussen KL, Milner GR, Delbey T, Skytte L, Søvsø M, Callesen F, Boldsen JL. Copper exposure in medieval and post-medieval Denmark and northern Germany: its relationship to residence location and social position. Heritage Sci. 2020;8:18.

38. Koizumi A, Azechi M, Shirawawa K, Saito N, Saito K, Shigehara N, et al. Reconstruction of human exposure to heavy metals using synchrotron radiation microbeams in prehistoric and modern humans. Environ Health Prev Med. 2009;14:52–9.
39. Lanzirotti A, Bianucci R, LeGeros R, Bromage TG, Giuffra V, Ferroglio E, et al. Assessing heavy metal exposure in Renaissance Europe using synchrotron microbeam techniques. J Archaeol Sci. 2014;52:204–17.
40. Rasmussen KL, Skytte L, Jensen AJ, Boldsen JL. Comparison of mercury and lead levels in the bones of rural and urban populations in southern Denmark and northern Germany during the Middle Ages. J Archaeol Sci Rep. 2015;3:358–70.
41. López-Costas O, Kylander M, Mattielli N, Álvarez-Fernández N, Pérez-Rodriguez M, Mighall T, et al. Human bones tell the story of atmospheric mercury and lead exposure at the edge of Roman World. Sci Total Environ. 2020;710:136319.
42. Milner GR, Boldsen JL. Transition analysis: a validation study with known-age modern American skeletons. Am J Phys Anthr. 2012;2012(148):98–110.
43. Aaron JE. Periosteal Sharpey's fibers: a novel bone matrix regulatory system? Front Endocrinol. 2012;3:98.
44. Al-Qtaitat A, Shore RC, Aaron JE. Structural changes in the ageing periosteum using collagen III immune-staining and chromium labelling as indicators. J Musculoskelet Neuronal Interact. 2010;10:112–23.
45. Kuo HW, Kuo SM, Chou CH, Lee TC. Determination of 14 elements in Taiwanese bones. Sci Total Environ. 2000;225:45–54.
46. Brodziak-Dopierala B, Kwapulinski J, Kusz D, Gajda Z, Sobczyk K. Interactions between concentrations of chemical elements in human femoral heads. Arch Environ Contam Toxicol. 2009;57:203–10.
47. Lambert JB, Simpson SV, Szpunar CB, Buikstra JE. Copper and barium as dietary discriminants: the effects of diagenesis. Archaeometry. 1984;26:131–8.
48. Lambert JB, Simpson SV, Szpunar CB, Buikstra JB. Bone diagenesis and dietary analysis. J Hum Evol. 1985;14:477–82.
49. Elliott TA, Grime GW. Examining the diagenetic alteration of human bone material from a range of archaeological burial sites using nuclear microscopy. Nucl Instrum Methods Phys Res B. 1993;77:537–47.
50. Guimarães D, Dias AA, Carvalho M, Carvalho ML, Santos JP, Henriques FR, Curate F, Pessanha S. Quantitative determinations and imaging in different structures of buried human bones from the XVIII–XIXth centuries by energy dispersive X-ray fluorescence—post-mortem evaluation. Talanta. 2016;155:107–15.
51. Grattan J, Abu Karaki L, Hine D, Toland H, Gilbertson D, Al-Saad Z, Pyatt B. Analyses of patterns of copper and lead mineralization in human skeletons excavated from an ancient mining and smelting centre in the Jordanian desert: a reconnaissance study. Min Mag. 2005;69:653–66.
52. Rasmussen KL, Skytte L, D'Imporzano P, Thomsen PO, Søvsø M, Boldsen JL. On the distribution of trace element concentrations in multiple bone elements in 10 Danish medieval and post-medieval individuals. Am J Phys Anthr. 2017;162:90–102.
53. Scharlotta I, Goriunova OI, Weber A. Micro-sampling of human bones for mobility studies: diagenetic impacts and potentials for elemental and isotopic research. J Archaeol Sci. 2013;40:4509–27.
54. Schoeninger MJ. Diet and status at Chalcatzingo: some empirical and technical aspects of strontium analysis. Am J Phys Anthr. 1979;51:295–310.
55. Burton JH, Price TD. The ratio of barium to strontium as a paleodietary indicator of consumption of marine resources. J Archaeol Sci. 1990;17:547–57.
56. Lugli F, Brunelli D, Cipriani A, Bosi G, Traversari M, Gruppioni G. C_4-plant foraging in northern Italy: stable isotopes, Sr/Ca and Ba/Ca data of human osteological samples from Roccapelago (16th–18th centuries AD). Archaeometry. 2017;59:1119–34.
57. Rasmussen KL, Delbey T, d'Imporzano P, Skytte L, Schiavone S, Torino M, Tarp P, Thomsen PO. Comparison of trace element chemistry in human bones interred in two private chapels attached to Franciscan friaries in Italy and Denmark—an investigation of social stratification in two medieval and post-medieval societies. Heritage Sci. 2020 (submitted).
58. Ysart G, Miller P, Crews H, Robb P, Baxter M, De L'Argy C, et al. Dietary exposure estimates of 30 elements from the UK total diet study. Food Addit Contam. 1999;16:391–403.
59. Rose M, Baxter M, Brereton N, Baskaran C. Dietary exposure to metals and other elements in the 2006 UK total diet study and some trends over the last 30 years. Food Addit Contam. 2010;27:1380–404.
60. Burton JH, Wright LE. Nonlinearity in the relationship between bone Sr/Ca and diet: paleodietary implications. Am J Phys Anthropol. 1995;96:273–82.
61. Allmäe R, Limbo-Simovart J, Heapost L, Verš E. The content of chemical elements in archaeological human bones as a source of nutrition research. Papers Anthropol. 2012;21:27–49.
62. Arrhenius B. Trace element analyses of human skulls. Laborativ Arkeologi. 1990;4:15–9.
63. Hunt JR, Vanderpool RA. Apparent copper absorption from a vegetarian diet. Am J Clin Nutr. 2001;74:803–7.
64. Bost M, Houdart S, Oberli M, Kalonji E, Huneau JF, Margaritis I. Dietary copper and human health: current evidence and unresolved issues. J Trace Elem Med Biol. 2016;35:107–15.
65. Taylor AA, Tsuji JS, Garry MR, McArdle ME, Goodfellow WL Jr, Adams WJ, et al. Critical review of exposure and effects: implications for setting regulatory health criteria for ingested copper. Environ Manag. 2020;65:131–59.
66. Grattan J, Huxley S, Karaki LA, Toland H, Gilbertson D, Pyatt B, et al. "Death more desirable than life"? The human skeletal record and toxicological implications of ancient copper mining and smelting in Wadi Faynan, southwestern Jordan. Toxicol Ind Health. 2002;18:297–307.
67. Koizumi A, Azechi M, Shirasawa K, Saito N, Saito K, Shigehara N, et al. Reconstruction of human exposure to heavy metals using synchrotron radiation microbeams in prehistoric and modern humans. Environ Health Prev Med. 2009;14:52–9.
68. Rabinowitz MB. Toxicokinetics of bone lead. Environ Health Perspect. 1991;91:33–7.
69. Gidlow DA. Lead toxicity. Occup Med. 2015;65:348–56.
70. Aufderheide AC, Neiman FD, Wittmers LE Jr, Rapp G. Lead in bone II: skeletal-lead content as an indicator of lifetime lead ingestion and the social correlates in an archaeological population. Am J Phys Anthropol. 1981;55:285–91.
71. Eda M, Kodama Y, Ishimaru E, Yoneda M. Lead concentration in archaeological animal remains from the Edo period, Japan: is the lead concentration in archaeological goose bone a reliable indicator of domestic birds? Int J Osteoarchaeol. 2013;24:265–71.
72. Nakashima T, Matsuno K, Matsushita T. Lifestyle-determined gender and hierarchical differences in the lead contamination of bones from a feudal town of the Edo period. J Occup Health. 2007;49:134–9.
73. Nakashima T, Matsuno K, Matsushita M, Matsushita T. Severe lead contamination among children of samurai families in Edo period Japan. J Archaeol Sci. 2011;38:23–8.
74. Scott SR, Shafer MM, Smith KE, Overdier JT, Cunliffe B, Stafford TW Jr, Farrell PM. Elevated lead exposure in Roman occupants of Londinium: new evidence from the archaeological record. Archaeometry. 2020;62:109–29.
75. Marshall JH, Liniecki J, Lloyd EL, Marotti G, Mays CW, Rundo J, et al. Alkaline earth metabolism in adult man. ICRP Publication 20. Oxford: Pergamon, 1973.
76. Hedges REM, Clement JG, Thomas CDL, O'Connell TC. Collagen turnover in the adult femoral mid-shaft: modelled from anthropogenic radiocarbon tracer measurements. Am J Phys Anthropol. 2007;133:808–16.
77. Shin JY, O'Connell T, Black S, Hedges R. Differentiating bone osteonal turnover rates by density fractionation; Validation using the bomb C14 atmospheric pulse. Radiocarbon. 2004;46:853–61.

Publisher's Note